ANALYSIS AND OPTIMIZATION OF ADHESIVELY BONDED JOINTS

by

Adnan Golubovic

Department of Mechanical Engineering

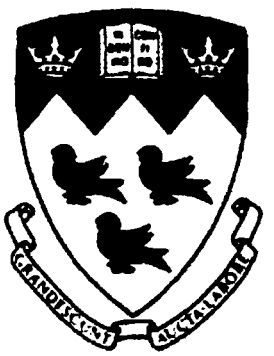

McGill University

Montreal, Quebec, Canada

April 2000

A report submitted to the Faculty of Graduate Studies and Research in partial fulfillment of the requirement of the degree of Master of Engineering

ABSTRACT

Metal and composite plates can be bonded together to form a joint known as the "single-lap" joint. The single-lap joint is studied under two different loading conditions: (i) out-of-plane load (bending) and (ii) in-plane load (tension). The different joint configurations are studied analytically and experimentally in order to achieve the optimum design. In configurations such as lap joints, the presence of stress singularities eliminates the possibility of using any stress-based failure criteria. A strain energy method is used to predict the strength of adhesively bonded joints because of its convergence with mesh refinement and it is found to be in good agreement with experimental results. Failure of single-lap joints is governed by the load case under consideration and the way in which the stress distribution varies at the joint ends. Failure varies with the taper angle (inner and outer), with or without additional epoxy beads. It is observed that designing the joint for one kind of load will not always be satisfactory because, for other load cases, different parameters will govern the design. It is shown that the optimum design for the single lap joint under bending loads will not be the optimum design for the tension case. Therefore, the optimum design can be chosen in a way that satisfies both loading conditions.

SOMMAIRE

Pour faire des connexions entre des plaques de métal et de matériaux composite, on peut utiliser une configuration qui s'appelle le "joint simple". Les joints simples sont étudiés sous deux conditions de chargement: (i) chargement hors plan (en flexion), et (ii) chargement dans le plan (en tension). Dans le but de trouver un design optimisé, les configurations de joints sont examinées théoriquement ainsi que par des essais mécaniques. Les configurations de joints simples démontrent des problèmes de concentration de contrainte, donnant lieu à des "singularités" lesquelles empêchent l'utilisation de critères de rupture basés sur telles contraintes. Pour éviter ce problème, un critère de rupture basé sur l'énergie de déformation (strain energy) est utilisé. Le résultat donne une convergence des prédictions avec le raffinement du maillage dans le programme d'analyse par éléments finis ainsi qu'une bonne corrélation avec les résultats des essais mécaniques. La rupture finale des joints simples dépend de la façon que l'on applique les forces et de la façon que l'on traite les extremités de la région d'adhésif entre les plaques de métal et de composite. Les variables qui sont importantes pour la rupture sont les angles d'amincisement des bouts de la plaque de métal, l'épaisseur de l'adhésif et la façon que l'on applique l'adhésif aux extremités de la région dudit adhésif. On observe que le meilleur design pour un chargement n'est pas nécessairement le meilleur design pour l'autre chargement. Autrement dit, le design optimisé pour le cas de flexion ne sera pas le design optimisé pour le cas de tension. Aussi, un design optimisé "général" peut être choisit, satisfaisant ainsi, plus ou moins, les deux conditions de chargement.

ACKNOWLEDGMENT

I would like to thank my advisor Professor Larry B. Lessard for his guidance, help and wisdom. Thank you Larry for your support and friendship.

I would like to thank Professor Jim Names who introduced me to the ABAQUS finite element package, and for his help and friendship.

I would like to say thank you to the people from the 265 office of the Macdonald Engineering Building.

Senada, thank you for always being with me.

TABLE OF CONTENTS

LIST OF FIGURES

LIST OF TABLES

LIST OF SYMBOLS

Symbol	Description
τ_m	Average Shear Stress in adhesive
P	Applied Load
b	Joint Width
l	Overlap Length
τ_x	Shear Stress
ω^2	Overlap Ratio
ψ	Adherend's Ratio
ϕ	Stiffness Ratio
X	Normalized Distance from Joint End respect to Overlap Length
G	Shear Modulus
E	Young's Modulus
ν	Poisson's Ratio
ν_{xy}	Interlaminar Poisson's Ratio
E_x	Longitudinal Tensile Modulus
E_y	Transverse Tensile Modulus
E_{xy}	Interlaminar Shear Modulus
X_T	Longitudinal Tensile Strength

X_C	Longitudinal Compression Strength
Y_T	Transverse Tensile Strength
Y_C	Transverse Compression Strength
S_{xy}	Interlaminar Shear Strength
S_{yz}	Transverse Interlaminar Shear Strength
S_{xz}	Longitudinal Interlaminar Shear Strength
t_1	Adherend (1) Thickness
t_2	Adherend (2) Thickness
t_3	Bondline Thickness
M_0	Bending Moment on the Adherend
k	Bending Moment Factor
σ_x	Axial Stress
σ_y	Peel Stress
σ_{xy}	Shear Stress
ρ	Density
v	Velocity Field Vector
U	Internal Energy per unit Mass
F	Body Force Vector
n	Normal Direction on Boundary
E_U	Internal Energy

E_K	Kinetic Energy
E_F	Energy dissipated between Contact Surfaces
E_W	Work done by External Force
E_S	Recoverable Elastic Strain Energy
$\dot{\varepsilon}$	Strain Rate
$\dot{\varepsilon}^{el}$	Elastic Strain Rate
α	Angle of an Inner Taper
β	Angle of an Outer Taper

Chapter 1

1 INTRODUCTION

1.1 INTRODUCTION TO COMPOSITE MATERIALS

The use of composite materials has been growing in many branches of industry, however, metals are still by far the most popular materials in many applications. With the growing use of composite materials, there is a simultaneously need for joining composite to metal parts. As one kind of composite material structure, bi-material lap joints have been widely used recently in various engineering applications such as in the aircraft and automotive industries, Ref. [1, 2, and 3]. Of the common forms of the lap joint, the single-lap joint (Fig. 1) is most widely used. Generally, currently existing single-lap joints are made of two plates joined by using either the mechanical connection method, or the solid-phase bonding process. The reasons why adhesive bonding in both metallic and composite material structures is desirable compared to other joining methods are:

- Number of production parts can be reduced, and design simplified
- Adhesive bonding provides a high strength to weight ratio

- Aerodynamic smoothness and improved visual appearance
- Use as a seal , or corrosion preventer when joining incompatible adherends
- Damping characteristics and noise reduction are superior to riveted or spot welded assemblies
- The adhesive is sufficiently flexible to allow for the variations in coefficient expansion when joining dissimilar materials

The single-lap joint is well known to be the most sensitive to changes in geometrical parameters (overlap length and thickness of the adhesive), compared with other joints. The eccentricity of the load path makes this simple joint a weak configuration. These geometrical parameters affect the performance of a bonded single-lap joint. Furthermore, it is well known that there are discontinuities of material and geometry at the bonding interfaces in this single-lap joint. These discontinuities cause singularities in the stress fields near the vertex of the bonding interfaces and very high stress concentrations. These stress concentrations may lead to delaminating initiation in the local area, and subsequently to global failure of joint structure. Among others, the issues of surface preparation, manufacturing methods and corrosion must be considered in the design of the joint.

1.2 LITERATURE REVIEW ON ADHESIVELY BONDED JOINTS

1.2.1 Analytical Analysis of Adhesively Bonded Joints

The classical paper published by Goland and Reissner [4] in 1944 is perhaps the most cited work in the analysis of adhesively bonded joints. In their work Goland and Reissner analyzed a single-lap joint for two limiting case, i.e., (i) where the adhesive layer is so thin that its effect on flexibility of joints can be neglected, and (ii) where the joint flexibility is mainly due to the adhesive layer (as is case of most thin-walled bonded

aerospace structures). During the analysis they assumed that (i) the axial stress in adhesive layer can be neglected, and (ii) normal and transverse shear stress in the adhesive layer do not vary across the thickness of the adhesive. Since the publication of Goland and Ressiner's work more than half a century ago, these basic assumptions have been employed by numerous authors to extend the work in the area of analysis and design of bonded joints. In [5] Pahoja tried to continue work of Goland and Reissner, and he considered the variation of the stress across the thickness of the adhesive. Pahoja described the behavior of the joint by linear, homogeneous, ordinary differential equations. Vinson [6] carried out extensive analytical work in the area of adhesively bonded joints involving composite adherends. Vinson also developed analytical tools to analyze adhesively bonded joints by including into the analysis the effects of transverse shear deformation, transverse normal strain, temperature and moisture variations. Adams [7, 8] predicted strength for lap joints especially with composite adherends by classical linear elastic solution. He also introduced Volkersen's shear leg equation that calculates shear stress in the adhesive.

The analytical analysis of adhesively bonded joints was simplified in most cases. The reason for simplification was the large number of the equations that had to be carried through the analysis, and the long time needed to complete the analysis. Today, there are fewer and fewer researchers that are analyzing adhesivley bonded joints using closed form solutions. Many are taking advantage of technology and analyzing adhesively bonded joints using the finite element method approach.

1.2.2 Analysis of Adhesively Bonded Joints by FEM

For the past three decades, researchers and engineers have been involved in the development of various techniques to analyze different kinds of bonded joints in composite structures. Efforts by the various groups have resulted in some useful computer programs that can be utilized by the engineers and designers engaged in bonded joint design work, Ref. [9]. One of the computer codes was written by Barthelemy, Kamat and Brinson [10]. They used higher order elements (eight-node) for their analysis

since the four-node element could not give good results. They used eight-node elements in order to manage high stress gradients that exist at the interface while analyzing the single-lap joint, thick adherend specimen and crack-lap joint. They indicated that the primary Young's modulus of the adherend, the overlap length, and adhesive material properties are the parameters most influential in optimizing the design of a single-lap joint.

Harris and Adams [11] used a non-linear finite element method to predict strength of a bonded single-lap joint. The finite element program that they used was able to account for the large displacements and rotations that occur in a single lap joint, and allowed the effects of elasto-plasticity in both the adhesive and adherends to be modeled. Adams and Atkins [12] considered the strength of CFRP/steel lap joints loaded in tension and performed a detailed stress analysis of the shear and transverse stresses in the joint. Adams [8] used finite elemant methods for elastic and elasto-plastic case to predict strength of lap joints with composite adherends. In [13] Hildebrand applied non-linear finite element methods in the analysis of single-lap joints between fibre-reinforced plastics (FRP) and metals in order to optimize the joint geometry. Kairouz and Cook [14] investigated the influence of bondline thickness and overlap length on the strength of bonded joints. Tsai and Morton [15] analyzed a single-lap joint with laminated polymeric composite adherends and with a spew fillet, subjected to tensile loading. They used finite element analysis for this problem to address the mechanics and deformation of such a material and bonding configuration.

Using the finite element approach, many researchers encountered problems trying to predict the strength of adhesively bonded joints because of stress singularities that exist if an interface results in a sharp corner. Therefore, a number of researchers have analyzed the stress singularity and displacement field near the vertex of this corner.

1.2.3 Stress Singularity

Extensive research on the stress singularity near the vertex of a bi-material wedge has been conducted [16-20]. Authors analyzed the plane problem of a composite body consisting of many dissimilar isotropic, homogeneous, and elastic wedges, perfectly bonded along their common interfaces. The particular behavior of the stress and displacement fields at the close vicinity of each interface corner is studied. The dependence of the order of singularity was established in relation with the mechanical properties of the wedges coalescing at the particular corner considered. Groth [21] analyzed stress singularities and fracture at the interface corners in bonded joints. He considered a number of possibilities for different crack shapes, sizes and crack locations that may be used in analysis. He showed some possible initial cracks or debond configurations at the terminus of an adhesive bonded joint with a spew fillet.

1.2.4 Fracture and Failure Modes of Fibre Composite Materials

Lessard [9] gives a summary on work done in area of adhesively bonded joints for different joint configurations. He also states that bonded composite joints can have three basic failure modes: (i) failure in the adherend, (ii) adhesive and (iii) failure of the adhesive or delamination of the adherend. Shorshorov and Gukasjan [22] analyzed two modes of fracture of fibre composite material: (i) cumulative (C-fracture) and (ii) noncumulative mode of fracture (NC-fracture). C-fracture mode is the mode when many fibers are pulled out from the matrix during fracture. NC-fracture corresponds to fracture of a fibre composite material that has very high interface strength.

1.2.5 Nondestructive Method of Evaluating Adhesive Bond Strength

Chapman [23] used two parameters to quantify the nondestructive inspection (NDI) of adhesive-lap joint bonds. The two indicators, local bond integrity index (LBI) and bond merit factor (BMF), were defined and their relationship to bond strength was demonstrated and discussed. The LBI indicator was obtained from readings of local bond integrity made with a commercial bond tester. The BMF was computed for the bondline region, using disbond detection data obtained for instrument sensitivity based on the LBI of the reference specimen. Williams and Wang [1] introduced ultrasonic and acoustic emission for nondestructive evaluation-characterization of flawed (undercure of the adhesive and excessive mold release on the adherends prior to bonding) and unflawed (proper cure of the adhesive) adhesively bonded fiber reinforced plastics.

1.2.6 Designing Bonded Joints

In his extensive work on bonded joints, Hart-Smith [2, 3, 24 and 25] has outlined various aspects of efficient bonded joint design in composite structures that an airframe designer should consider while designing bonded joints between components. Hart-Smith has also made many useful studies to analyze the load transfer mechanism in the adhesive bonded joints and outlined some practical ways to minimize the transverse shear and peel stresses in the adhesive layer. Renton and Winson [26] studied the numerous parameters that influencing the stress distribution within the adhesive of a single-lap joint. Their study included transverse shear and normal strain deformations. They analyzed both isotropic and anisotropic material systems of similar or dissimilar adherends. Greszezuk and Macander [27] tested scarf joint under tension, compression and fatigue load. Their results showed that the compressive strength of the scarf joint to be proportional to the scarf tip thickness, with joint strength increasing as the scarf tip thickness decreases. The text by Adams and Wake [28] presents a comprehensive treatise on the design and production of adhesively bonded joints used as primary load carrying members. The mechanics and

chemistry of bonded joints are discussed, and standard methods of testing adhesives are outlined.

1.2.7 Surface Pretreatment for Bonding

Adhesive bond durability depends on the properties of the adhesive, the surface preparation, and the primer used. Surface pretreatment is necessary in order to substitute pre existing weak oxide layer on the metal surface with suitable one.

In [29] Galantucci et. al. worked on surface treatment to improve mechanical resistance for adhesive bonding of plastic composites reinforced with fibers and metallic material using an excimer laser. Arnold and Sanders [30] studied titanium surface pretreatment for bonding with polyimide and epoxy adhesives. They used chromic acid anodizing for pretreatment on titanium surface prior to bonding.

As one can notice, the analysis of adhesively bonded joints is not that old (since 1944), and so far extensive analysis has been performed in this area. The literature review covers most of the problems that one could encounter during the analysis and design of adhesively bonded joints but still, adhesively bonded joints are not analyzed completely. In the literature, the overlap length, adhesive thickness, stress singularities, surface preparation before bonding, testing and other parameters are studied in many different ways, but further research is needed to improve joint design and increase the strength of the adhesively bonded joints. The present analysis on optimization of adhesively bonded joints is limited because of the presence of stress singularities near the vertex. Because of this phenomena, the finite element method is not a powerful tool for structural analysis. Therefore, there is a particular need for research into adequate failure criteria that are not influenced by mesh refinement and stress singularities.

1.3 OBJECTIVE

The objective of this research is to optimize the design of the joint ends of single-lap joints between composite material and metals (titanium) in order to increase joint strength. Optimization has to be carried out for a single-lap joint subjected to two different loading conditions that are applied alternatively:

(i) Single-lap joint under concentrated out-of-plane load (bending) and

(ii) Single-lap joint under in-plane load (tension)

1.4 THESIS OVERVIEW

In Chapter 2, different failure criteria and strength predictions for adhesively bonded joints are studied. Different lap geometries are presented. A simple single-lap joint without any geometry changes at the ends is accepted as a baseline model. Theoretical stress singularities prevented use of stress- based failure criteria and strain energy is proposed as failure criteria because it converges with mesh refinement.

In Chapter 3, finite element model is developed using a commercial finite element code. The finite element baseline model, the single-lap joint without taper, is modeled for two loading conditions: (i) single-lap joint under out-of-plane load and (ii) single-lap joint under tension. New models are created with different geometries of the model, i.e., outer and inner tapers, and these are compared to the baseline model. Their efficiency is determined from these comparisons. The plain strain analysis is performed using ABAQUS finite element code with linear elastic material properties.

In Chapter 4, three-point bending and tension tests are performed for different joint configurations. The results obtained from experimental work are used to evaluate a finite element model and verify proposed failure criteria. Different load cells are used for

measuring failure load of a single-lap joint since these structures are more sensitive to out-of-plane load than to in-plane load.

In Chapter 5, result of the experimental and finite element analysis for single-lap joints under out-of-plane and tension loads are presented. Comparing the baseline model with the best result shows the order of magnitude of possible improvements.

Chapter 6 concludes present study with design recommendations for a single-lap joint under different loading conditions and gives recommendations for future studies in this field.

Chapter 2

2 DESIGN OF ADHESIVELY BONDED JOINTS

2.1 BONDED JOINT CONFIGURATIONS

The design and analysis of adhesively bonded joints is very complex. If an analytical approach is used, it involves at least 26 equation and 26 unknowns, and after the roots of the equations are found, computer program such as BOND 4 is needed to do design analysis or optimization studies, Ref. [5, 10]. Computer programs listed in [9] have different assumptions, and concern different configurations. For very simplified preliminary study some general design recommendations can be made on different joint configurations:

Figure 1: Single-Lap Joint

Single-lap joints (Fig. 1) have the simplest configuration and they are efficient at transferring in-plane shear. These joints should not be used for compression loads unless the joint is stabilized because the eccentricity increases in compression.

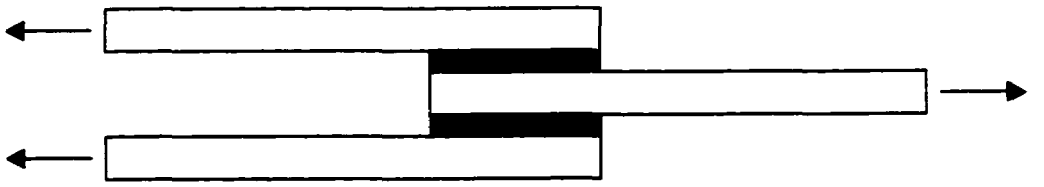

Figure 2: Double-Lap Joint

Double-lap joints (Fig. 2), which are essentially two single-laps back-to-back, can be used to eliminate joint rotation because there is no net bending moment on a central adherend but the outer adherends have. This moment is giving rise to tensile stresses across the adhesive layer at the end of the overlap where they are not loaded and compressive stresses at the end where they are loaded.

Figure 3: Stepped-Lap Joint

Stepped-Lap Joints (Fig. 3) achieve higher average shear stress than the scarf joint (Fig.4); also the strength of stepped lap joint is not sensitive to the number of steps when the total lap length is held constant. Scarf and stepped lap joints are lighter in weight than any other lap joints at all load levels. It should be noted that as the number of steps increase the stepped lap joint approaches the scarf joint configuration.

Figure 4: Scarf Joint

The Scarf Joint (Fig. 4) has its advantage in aerodynamic smoothness, but disadvantage is in the careful machining required to have a uniform bond line, so it is more useful for metallic adherends rather than those composed of composite materials. Ref. [27] states that the scarf joint approaches the ideals of strain compatibility in the adherends and uniform stress in the adhesive. One result of this is that ductility in scarf joints is less important than in any other joint configuratio

The design of adhesively bonded joint was extensively studied in Ref. [2, 3, and 26] and the design recommendations that are accepted from those references are:

• Whenever it is possible, one should join identical adherends of a like geometrical configuration. For dissimilar adherends, this can be accomplished by equalizing the in-plane and bending stiffness parameters. This minimizes the skewing of the adhesive peak shear and normal stresses and shear concentration at the edges of the joint that can lead to premature adherend failure.

• Use material systems with relatively high values of primary modulus (Q_{11}). Such a system minimizes peak stress levels, yielding a more uniform adhesive shear stress distribution. When the adherends have relatively low values of Q_{11}, increasing the adherend thickness can minimize the adhesive stress peaks.

• Use an overlap length of about ten times the minimum thickness adherend. This gives a more uniform adhesive shear stress distribution without causing the failure mode to shift into the adherend. (Renton and Winson recommend this in Ref. [26] where they also have shown that for about 15 and 20 mm overlap length, there is very little change in shear stress distribution in the overlap region. Hart-Smith in Ref. [3] states that experience has shown that the best adhesive bonds have a thickness ranging from 0.12 to 0.25 mm. If one choses larger values for adhisive thickness, it tends to reduce the stiffness of the adhesive).

• The joint's intended loading history should influence the selection of the adhesive. If static, the adhesive should posses relatively high tensile and shear ultimate strength values. If the application is that of fatigue, the fracture toughness of the adhesive must be an added consideration.

• If the adherend is laminated, the bending-stretching coupling matrix ([B]) should be zero.

2.2 STRENGTH PREDICTIONS FOR LAP JOINTS

The type of failure one observes in a bonded joint is dependent on whether the joint is experiencing a static or fatigue loading condition. For example, while a given joint may fail in the adhesive due to peak shear and normal stresses at ultimate load, it very possibly could fail in fatigue in the adherend due to a high moment concentration factor at the edge of a joint induced by the joint eccentricity. Such failure would depend on the materials being used, the mean fatigue load and fatigue stress ratio under which adherend is experiencing. Hypothetically, an adhesive bonded joint may fail due to static or fatigue loads in three distinct modes. The adhesive may fail due to high shear and normal stresses. The adherends may fail due to an axial load coupled with too large moment at joint edge or if the adherends are laminated, a ply in adherend near the joint can fail by resin deterioration due to high interlaminar stresses.

Lessard in [9] categorized joints according to their failure, where he states that the strongest joint is achieved when failure is at 100% of the adherend strength. The next strongest joint fails in the adhesive or in the interface and this is the mode that the joint normally fails. In the final category, the poorest design of the joint fails under peel loads as failure of the adhesive or as delamination of the adherend.

In the next section, three different failure analyses for the single-lap joint (joint that fails in the adhesive or interface) will be introduced:

(i) Algebraic solution

(ii) Stress criteria (FEM)

(iii) Strain energy method (FEM)

2.2.1 Linear Closed Form Algebraic Solution

The average shear stress τ for a simple lap joint is given by

$$\tau_m = \frac{P}{bl} \tag{1}$$

where P is applied load, b is joint width, and l is overlap length. Often a large factor of safety (at least 10) is used and, and it is not surprising that joint is strong enough. This is, of course rather simplistic and takes no account of the flexibility of the adhesive and adherends. Adams in [7] introduced Volkersen's shear lag equation that was used to analyze the stresses in riveted panels, but could only deal with the case of an infinite number of tiny rivets, which effectively created a continuum and this continuum is identical to the case of an adhesive layer. Volkersen assumed that the adhesive deformed only in shear and the adherends deformed only in tension. According to Volkersen, the ratio of the shear stress τ_x at any position X from one edge of the joint to the average applied shear stress ($\tau_m = \frac{P}{bl}$) is given by equation (2) and results are presented in Fig. 5.

$$\frac{\tau_x}{\tau_m} = \frac{\omega}{2}\frac{\cosh \omega X}{\sinh \frac{\omega}{2}} + \left(\frac{\psi - 1}{\psi + 1}\right)\frac{\omega}{2}\frac{\sinh \omega X}{\cosh \frac{\omega}{2}} \tag{2}$$

where

$\omega^2 = (1+\psi)\phi$

$\psi = \frac{t_1}{t_2}$

$\phi = \frac{Gl^2}{Et_1t_3}$

$X = \frac{x}{l}$

$\frac{\tau_x}{\tau_m}$ = Stress coefficient

ω^2 = Overlap ratio

ψ = Adherend's ratio

ϕ = Stiffness ratio at the interface

X = Normalized distance from joint end respect to overlap length, Fig. 6

G = Shear modulus of adhesive

E = Young's modulus of the adherends

t_1, t_2 = Thickness of the adherends

t_3 = Thickness of the joint

l = Length of the joint

Volkersen neglected several important factors. First, because the directions of the two forces in Fig. 1 are not collinear, there must be a bending moment applied in addition to the in-plane tension. The adherends bend and the rotation alters the direction of the load line in the region of the overlap to form a geometrically non-liner problem. Thus, joint displacements are no longer directly proportional to the applied load. Goland and Reissner [4] took this effect into account by using a bending moment factor, k, which relates the bending moment on the adherend at the end of the overlap, M_0, to the in-plane loading, by relationship,

$$M_0 = \frac{kPt_3}{2} \tag{3}$$

Where t is the adherend thickness (the thickness of the adhesive layer was neglected). If the load on the joint is very small, no rotation of the overlap takes place, so $M_0 = \frac{Pt_3}{2}$ and k=1.0. As the load is increased, the overlap rotates, bringing the line of action closer to the centerline of the adherends, thus reducing the value of the bending moment factor. The classical work of Volkersen, Goland and Reissner [4] was limited because peel and shear stresses were assumed constant across the adhesive thickness, the shear was

maximum and not zero at the overlap end and shear deformation of the adherends was neglected, Fig. 5. Because the end face of the adhesive is a free surface, there can be no shear stress on it. Thus, by the law of complementary shears, the τ_x shear stress at the joint must also be zero.

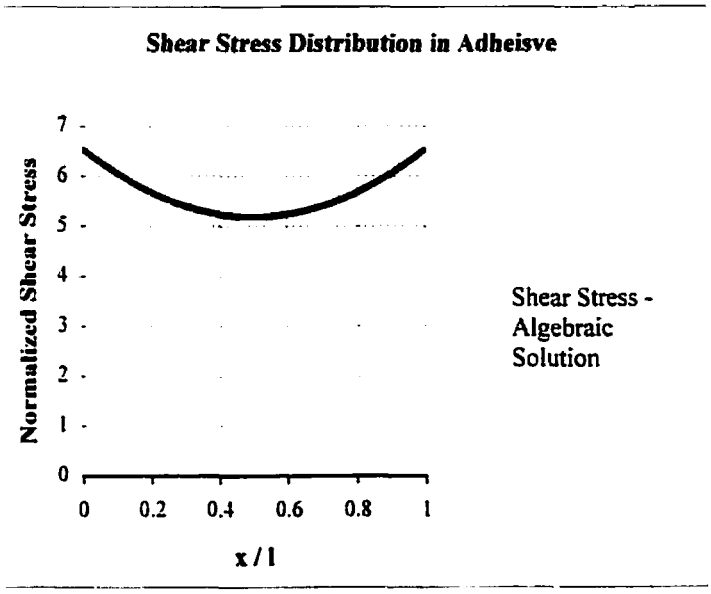

Figure 5: Shear stress distribution in adhesive (Algebraic Solution)
(Shear stress normalized with respect to the shear strength)

2.2.2 Finite Element Methods

The finite element method (FEM) is now a well-established means for mathematically modeling stress (and many other) problems. Its advantage lies in the fact that the stresses in a body of almost any geometrical shape under any load can be determined. In [8] Adams used (i) maximum stress and (ii) maximum strain criteria to predict strength of adhesively bonded joint under quasi-static loading. In [12] Adams and Atkins used (i) maximum principal stress criteria to predict strength of the joint. Hildebrand [13] analyzed adhesively bonded joints and he used the same failure criteria (Tsai-Wu) for the adhesive and composite adherend.

Analyzing joints by FEM between two or three dissimilar materials that have sharp corners (single-lap joint) will produce stress singularities in those locations. Mesh refinement appears to have a great effect on stresses calculated at the attachment, as they continue to increase with continued mesh refinement. Theoretically the stress is infinite at this location and therefore increasing the mesh density will not produce a converged stress value at this location. The main stress components over interface region (titanium-adhesive Fig. 6) were examined in Figs. 7-15, from finite element analysis performed by the author. Different element ratios were investigated and its influence on stress values at locations where stress singularities appeared. Finite element analysis with mesh distribution, element type and dimensions of a single lap joint are discussed in detail in Chapter 3 (section 3.2).

For very coarse mesh (element ratio 0.01) under external tension force of 4 KN the value of axial stress at the vertex was under Yield stress value of the adhesive, Fig. 7. With mesh refinement (element ratio 0.25) axial stress at the vertex is almost two times greater than the stress value obtained from the more coarse mesh, Fig.8. For element ratio 0.5, stress values increased to almost three times the value obtained for the coarse mesh, Fig. 7 and Fig. 9. For peel stress values at the vertex even greater differences were found. For element ratio 0.5 peel stress values at the vertex are almost five times greater than peel stress values for element ratio 0.01, Fig. 10 and Fig. 12. In the case of shear stresses, the fine mesh produced two times greater values at the vertex than for the coarse mesh. Fig. 13 and Fig. 15.

Comparing stress results that were obtained from algebraic solution (Fig.5) with the stresses obtained from most coarse mesh (0.01 element ratio, Fig. 13) one can notice that peak value for algebraic solution is six times grater than values obtained from FEM. From Fig. 5, notice that the shear stress distribution in the middle of overlap region is not close to the zero, and it has almost five times greater value than FEM where the variation of the stresses through thickness is considered and also adherends are deformed in bending. Algebraic solution has limitation for its application and can be only used for rough calculation. Therefore, one have to consider FEM approach in order to find stress

distribution in the adhesive, but then there is a problem to predict strength of the adhesively bonded joints. Analyzing the stress values obtained from the current analysis, it is obvious that if one used a stress-based failure criteria, there will be error and this error is obviously influenced by mesh refinement.

Stress Singularity

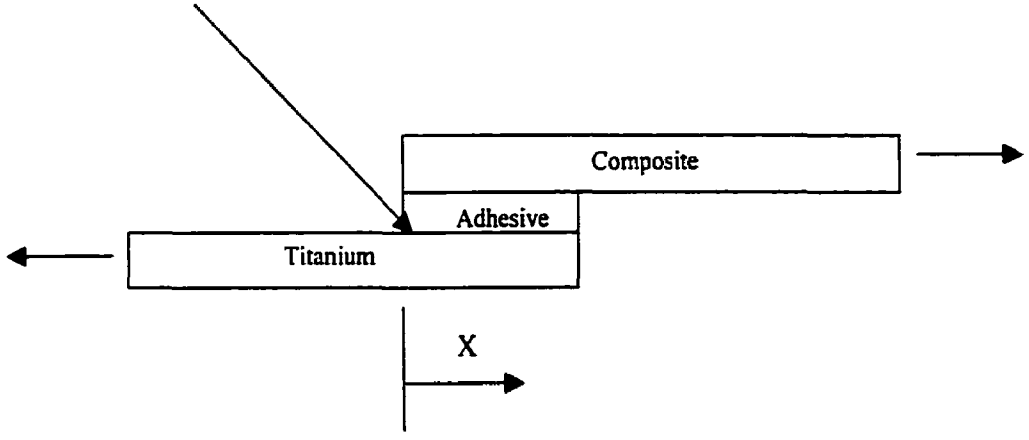

Figure 6: Single-Lap Joint with overlap region l = 20 mm

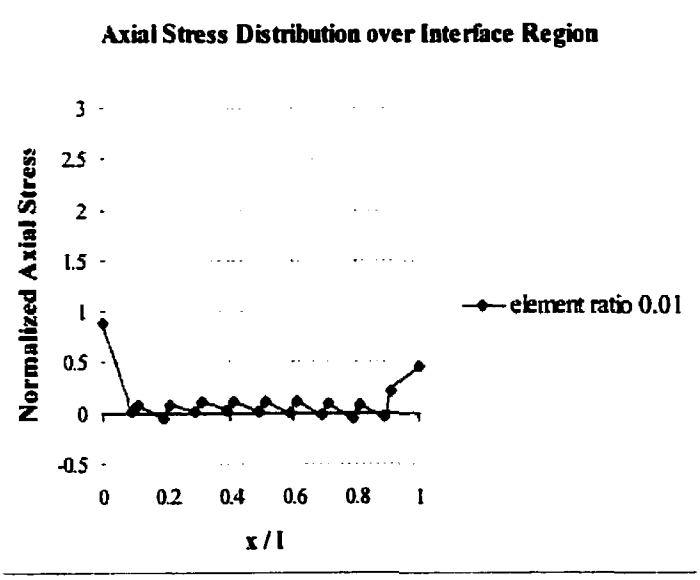

Figure 7: Axial stress distribution over interface for element ratio 0.01 (Axial stress normalized with respect to tensile strength)

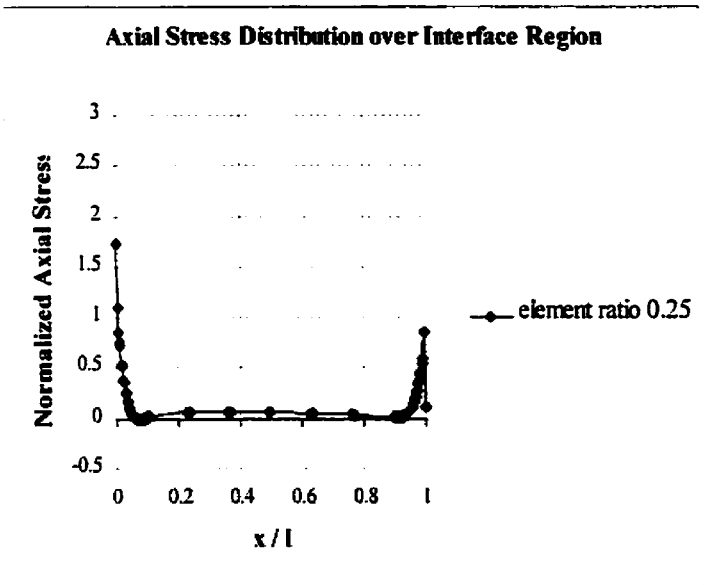

Figure 8: Axial stress distribution over interface for element ratio 0.25 (Axial stress normalized with respect to tensile strength)

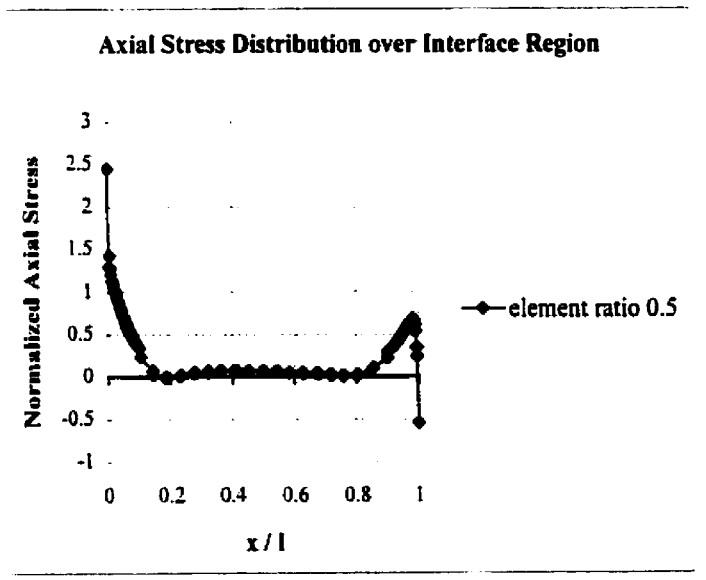

Figure 9: Axial stress distribution over interface for element ratio 0.5 (Axial stress normalized with respect to tensile strength)

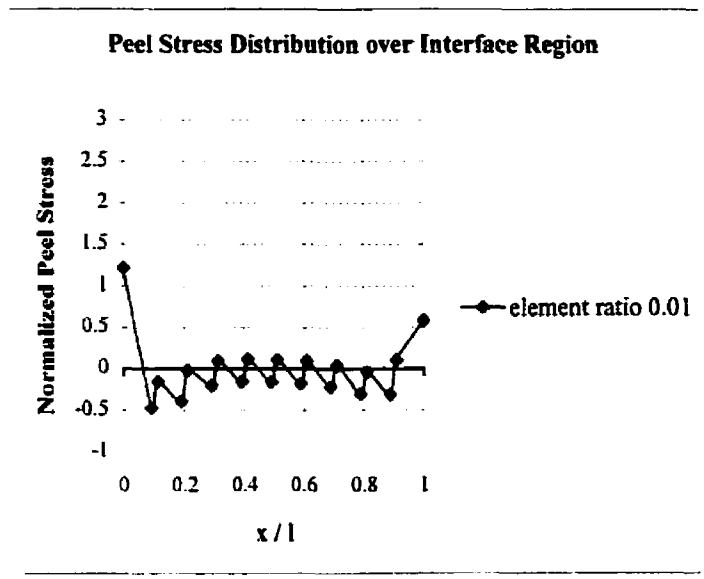

Figure 10: Peel stress distribution over interface for element ratio 0.01
(Peel stress normalized with respect to tensile strength)

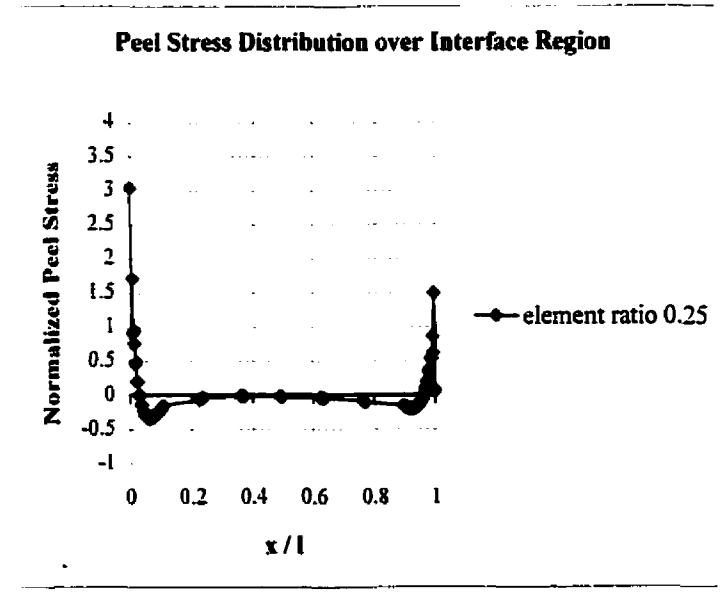

Figure 11: Peel stress distribution over interface for element ratio 0.25
(Peel stress normalized with respect to tensile strength)

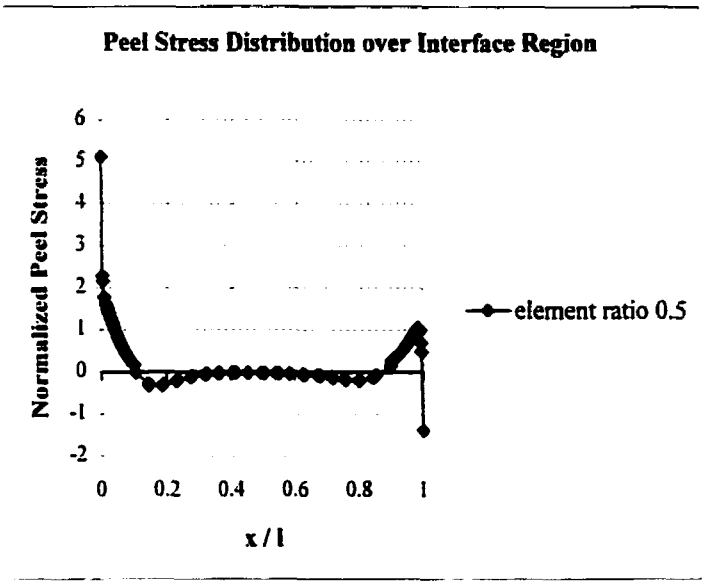

Figure 12: Peel stress distribution over interface for element ratio 0.5
(Peel stress normalized with respect to tensile strength)

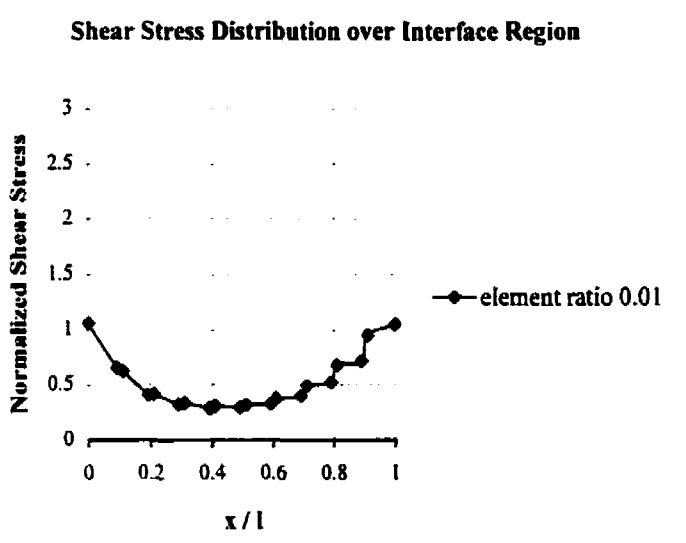

Figure 13: Shear stress distribution over interface for element ratio 0.01
(Shear stress normalized with respect to shear strength)

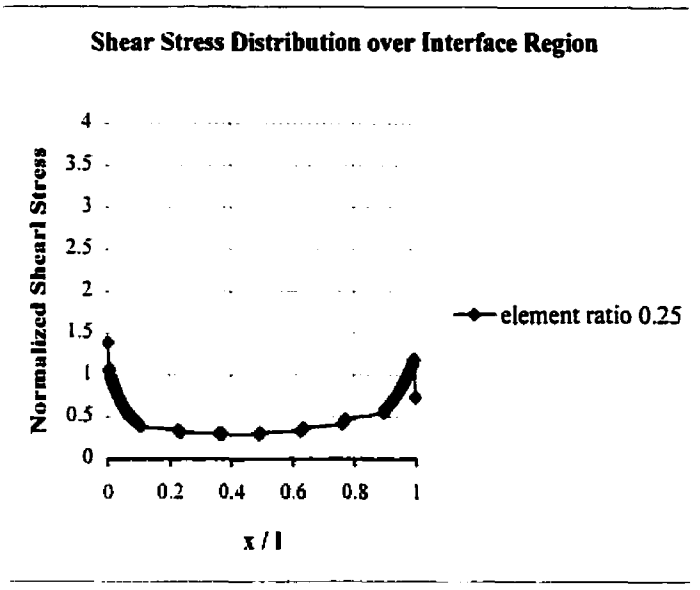

Figure 14: Shear stress distribution over interface for element ratio 0.25 (Shear stress normalized with respect to shear strength)

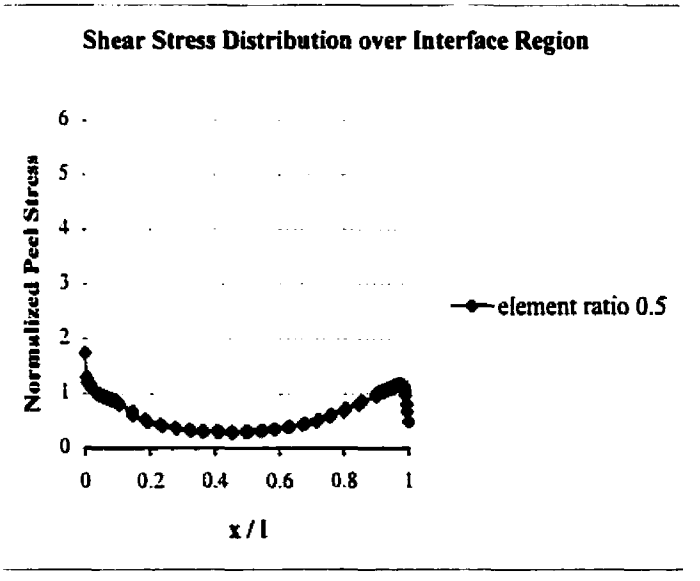

Figure 15: Shear stress distribution over interface for element ratio 0.5 (Shear stress normalized with respect to shear strength)

2.2.3 Energy Balance Method used in ABAQUS Code

It has been shown that the use of stress-based failure criteria will produce error that obviously depends on the mesh density (more dense mesh will give larger stresses at the stress singularity locations). There was a need to find a failure parameter that does not depend on mesh density. ABAQUS finite element code has an option to output the strain energy for the elements that are of user interest, and it has been found that this value converges with mesh refinement. ABAQUS finite element code also has the capability to analyze different problems that can involve static or dynamic analysis with elastic or plastic material modeling. The next step will introduce the equations that ABAQUS uses in order to calculate the strain energy. In the present analysis the loading is static and material is modeled as elastic, so that this will cancel out a number of terms from the equations that are initially introduced.

The conservation of energy implied by first law of thermodynamics states: "The time rate of change of kinetic energy and internal energy for a fixed body of material is equal to the sum of the rate work done by the surface and body forces". In ABAQUS this is expressed as:

$$\frac{d}{dt}\int_{v}\left(\frac{1}{2}\rho\, v\cdot v+\rho U\right)dV=\int_{s} v\cdot t\,dS+\int_{v} f\cdot v\,dV \tag{4}$$

Where

ρ	is the current density;
v	is the velocity field vector,
U	is the internal energy per unit mass,
t	is the body force vector, $t=\sigma\cdot n$, and
n	is the normal direction vector on boundary S is stress tensor

An energy balance for the entire model can be written as:

$$E_U+E_K+E_F-E_W=\text{Constant} \tag{5}$$

Where

E_U is internal energy

E_K is kinetic energy

E_F is energy dissipated by friction

E_W is work done by external forces

In the present model the conservation of energy implied by first law of thermodynamics states that the time rate of change of internal energy for a fixed body of material is equal to the sum of the rate work done by surface forces ($E_U - E_W$ = *constant and* $E_K = E_F = 0$).

With elastic material properties the total strain rate is equal to the elastic strain rate ($\dot{\varepsilon} = \dot{\varepsilon}^{el}$) *and internal energy is equal to the recoverable elastic strain energy* ($E_U = E_S$). *ABAQUS makes it possible to output elastic strain energy* (E_S) *for specified elements that are of user inters and this output has to be specified in ABAQUS input file (Appendix A).*

For the present model, recoverable elastic strain energy (E_S) of adhesive is obtained as an output form the ABAQUS finite element code for three different element ratios, Fig. 16. The element ratios were the same as those used to calculate the stress distribution at the joint interface (Figs. 7 – 15).

The value of recoverable elastic strain energy obtained for element ratio 0.01 and external force of 4 KN in tension is 1.175E-02 J. For element ratios 0.25 and 0.5, under same loading conditions as for 0.01, the value of recoverable elastic strain energy is equal to 1.18E-2 J, Fig. 16, essentially identical.

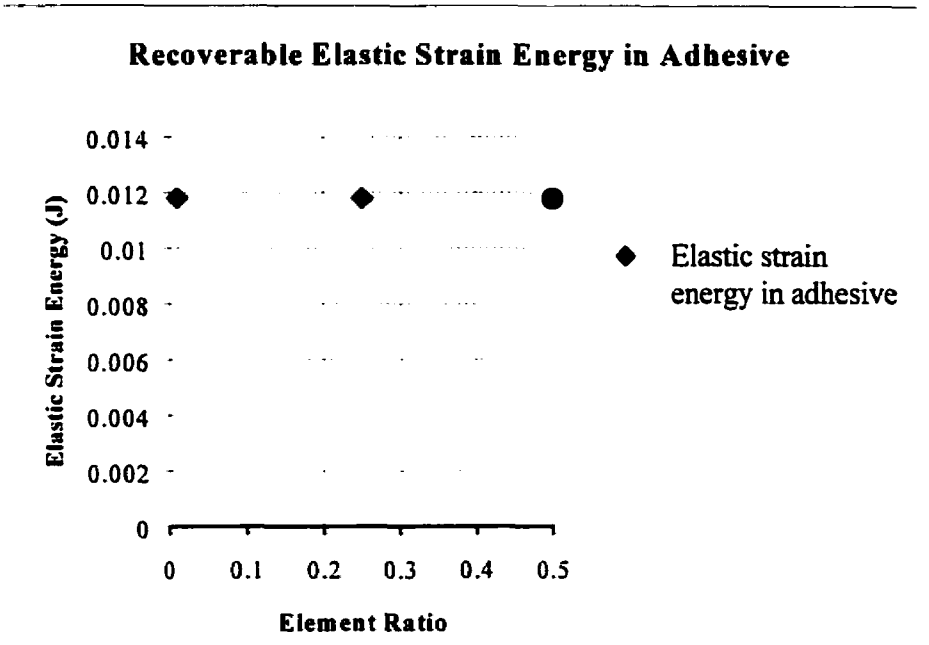

Figure 16: Elastic Strain Energy in the adhesive for different element ratios

The elastic strain energy obtained for the overlap adhesive converged with mesh refinement, Fig. 16. A simple single-lap joint is accepted as the baseline model, Fig. 6, and the adhesive strain energy obtained for this joint is accepted as a reference value. If one examines different geometry shapes of a single-lap joint under the same loading condition, different stress-strain fields in the adhesive will be obtained and with this, elastic strain energy will vary. The value for elastic strain energy can be:

(i) equal to the value obtained for baseline model
(ii) less than value obtained for baseline model
(iii) greater than value obtained for baseline mode

• If the value for elastic strain energy is equal to the value that is obtained for baseline model, the design did not get better nor worse.

• If the value for elastic strain energy is less than value obtained for baseline model, the design is improved (stresses and strains decreased in the adhesive).

- If the value for elastic strain energy is greater than value obtained for baseline model, the design solution did not improve. On the contrary, it has a worse solution (stresses and strains increased in the adhesive).

Values of elastic strain energy that are obtained for different design shapes of a single-lap joints and design recommendations on best possible design for a single-lap joint under different loading conditions are presented in Chapter 5 and Chapter 6.

Chapter 3

3 FINITE ELEMENT MODEL

3.1 DESCRIPTION OF THE JOINT

For both loading cases (tension and out-of-plane load) finite element analysis has been performed. For joining titanium plates, 0.12 m x 0.0254 m x 0.001 m, and composite plates, $[0_4/90_4]_s$ with 0.146 mm ply thickness, bonding recommendations have been taken from Ref. [2, 3, 13 and 26], Fig. 17. In Ref. [26], it has been shown that there is a length of bond line, tested in tension, beyond which no load capacity increase occurs, due to the nature of the shear stress distribution. Ref.[3, 26] states that the best overlap length is equal to 0.02 m for the type of the joint that is used in this analysis. Ref. [3] also states that 0.12 - 0.25 mm thickness of the joint adhesive shows the best results in practice. Further modeling is concentrated on the geometry of the joint ends. The effects of the ends are crucial for the strength of a single-lap joint due to the combination of high tensile, peeling and shearing stresses. Different kinds of tapering are examined:

(i) Inner taper at the metal adherend, Fig. 18 and Ref. [13]

(ii) Outer taper on the metal adherend, Fig.19 and Ref. [2]

(iii) Inner taper on the metal adherend with combination of outer adhesive fillets, Fig. 20 and Ref. [13]

Inner taper refers to a taper on the titanium adherend, meaning that the extra space will be filled with adhesive (Fig. 18). Outer beads are designed only with 45^0 angles and they have been combined with inner tapers (Fig. 20). Inner taper is defined by an angle α, where $\tan\alpha = \frac{b}{d}$ (Fig. 18) and outer taper is defined by an angle β where $\tan\beta = \frac{c}{d}$ (Fig. 19). For modeling inner and outer tapers, variable **d** varies from 0 to 20 mm, whereas variables **b** and **c** have three values: (i) 0.5 mm, (ii) 0.75 mm and (iii) 0.9 mm. From the values of **b**, **c** and **d** angles for inner and outer tapers are calculated (Tables 1 and 2)

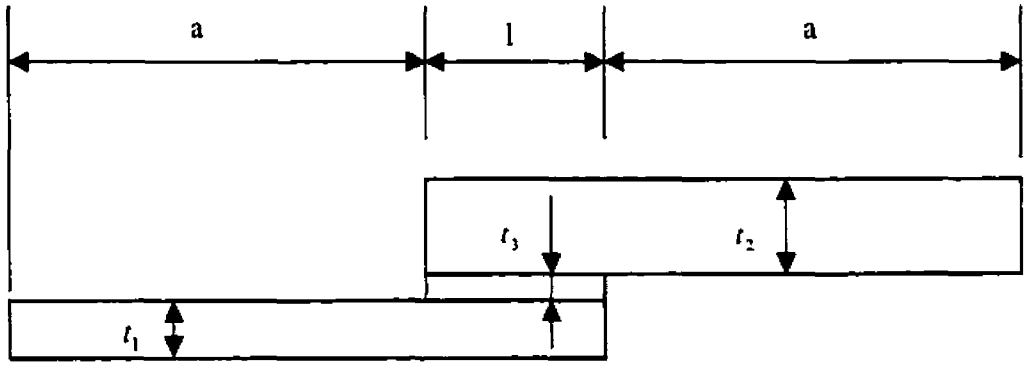

a = 0.10 m, l = 0.02 m, t_1 = 0.001 m (titanium), t_2 = 0.0023 m (composite),

t_3 = 0.00015 m (adhesive)

Figure 17: Geometry of the Single - Lap joint; Baseline model

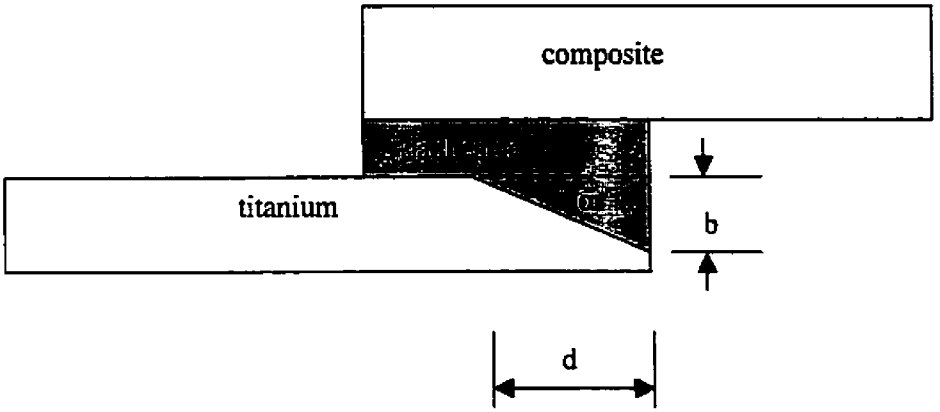

Figure 18: Inner taper with an α angle

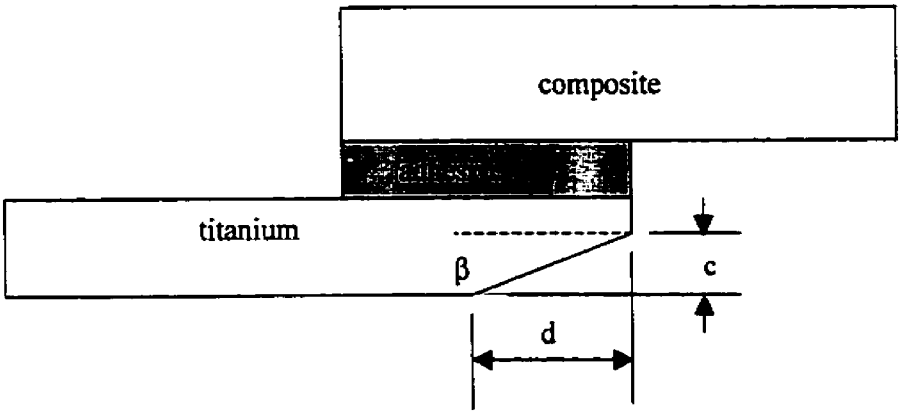

Figure 19: Outer taper with a β angle

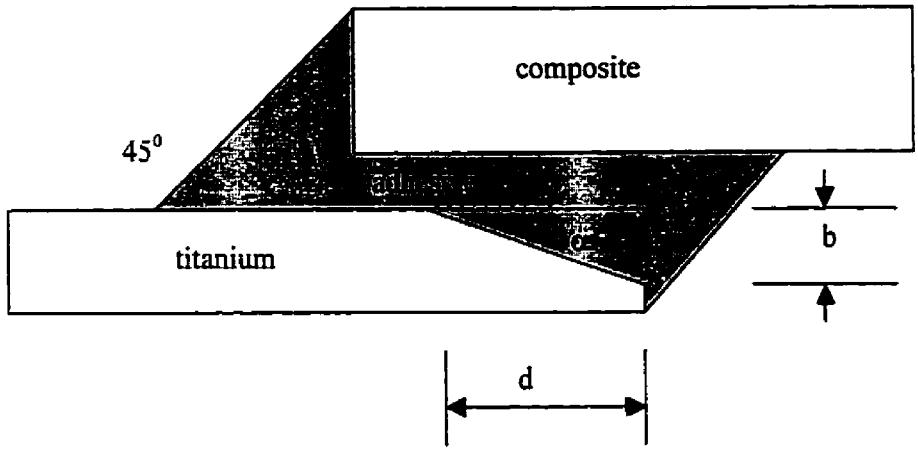

Figure 20: Inner taper with outer bead of 45 degrees

Variable d (mm)	Angle α (°) with b=0.5 mm	Angle α (°) with b=0.75 mm	Angle α (°) with b=0.9 mm
0	0	0	0
2	14	20.55	24.22
4	7.12	10.61	12.68
6	4.76	7.12	8.53
8	3.57	5.35	6.41
10	2.86	4.28	5.14
12	2.38	3.57	4.28
14	2.04	3.06	3.67
16	1.79	2.68	3.21
18	1.59	2.38	2.86
20	1.43	2.14	2.57

Table 1: The angle of inner taper, angle α (°)

Variable d (mm)	Angle β (°) with c=0.5 mm	Angle β (°) with c=0.75 mm	Angle β (°) with c=0.9 mm
0	0	0	0
2	14	20.55	24.22
4	7.12	10.61	12.68
6	4.76	7.12	8.53
8	3.57	5.35	6.41
10	2.86	4.28	5.14
12	2.38	3.57	4.28
14	2.04	3.06	3.67
16	1.79	2.68	3.21
18	1.59	2.38	2.86
20	1.43	2.14	2.57

Table 2: The angle of outer taper, angle β (°)

3.2 DESCRIPTION OF FINITE ELEMENT ANALYSIS

The single lap joint, from Fig. 17, was modeled using three different finite element meshes, Figs. 22-27. The stress state is relatively constant in the width direction, therefore the problem is considered as a two-dimensional one. The meshes were generated using eight-node quadrilateral 2D plain strain solid elements (type CPE8R). Six elements were used through thickness of the adhesive, sixteen for the composite and also sixteen for the titanium. The analysis assumed linear elastic material properties, Tables 3, 4, and 5 and Ref. [31]. In the analysis of asymmetric joints, such as the single-lap joint, it is important to take geometric non-linearity (changing geometry under loading) into account. Joint rotation changes the stress distributions in the adherends and the adhesive under loading. Thus geometric non-linearity is included in this model. Three different mesh types (0.001, 0.25 and 0.5 element ratio) are used to show that: (i) stresses in the adhesive do not converge with mesh refinement and (ii) strain energy of the adhesive converges with mesh refinement. The baseline model, the simple single-lap joint in Fig. 17, is relatively long and thin such that the mesh for entire model is very

difficult to display. Therefore, only regions that are characteristic for this kind of problem are displayed (region A and region B, Fig. 21). Since it has been shown that elastic strain energy of the adhesive converged with mesh refinement, Fig. 16, 0.5 element ratio is used to generate the mesh for the joint geometry that is shown in Figs. 18, 19, and 20 (single-lap joint under out-of-plane load and single-lap joint under tension). In order to create outer tapers, Fig. 19, elements in the β region, that have titanium material properties in the case of simple single-lap joints, have to be removed. If one wants to create inner taper Fig. 18, elements in the α region, that have titanium material properties in the case of simple single-lap joints, have to be replaced with elements that have adhesive material properties. Outer beads of 45 degrees are modeled using extra elements distributed in the way that is shown in Figs. 28 and 29.

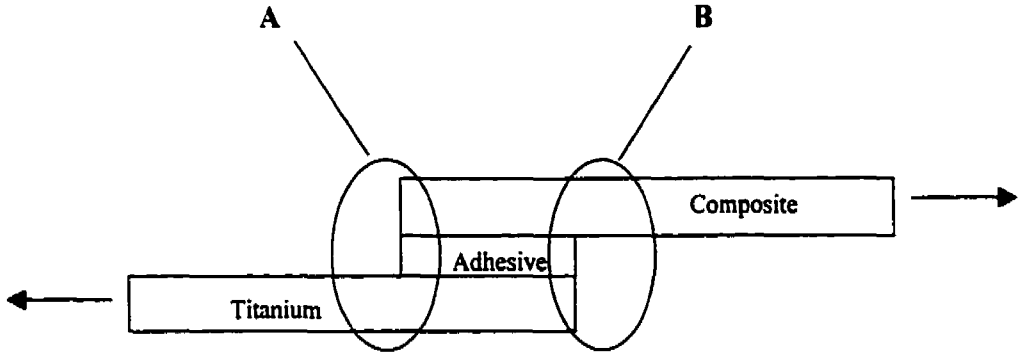

Figure 21: Stress Singularity Regions in a Single-Lap Joint

Material property	Unit	Value
Young's modulus	GPa	114
Poisson's ratio	-	0.33
Shear modulus	GPa	43

Table 3: Titanium material properties

Material property	Unit	Value
Young's modulus	MPa	689
Shear strength	MPa	15
Tensile strength	MPa	12
Poisson's ratio	-	0.33
Shear modulus	MPa	259

Table 4: Depend 330 adhesive properties

Material property	Unit	Value
Longitudinal tensile modulus	GPa	147
Transverse tensile modulus	GPa	9
Interlaminar shear modulus	GPa	5
Interlaminar Poisson's ratio	-	0.3
Longitudinal tensile strength	MPa	2004
Longitudinal compress. strength	MPa	1197
Transverse tensile strength	MPa	53
Transverse compression strength	MPa	204
Interlaminar shear strength	MPa	137
Transv. Interlaminar shear strength	MPa	42
Ply thickness	mm	0.146

Table 5: Material properties for graphite / composite AS4/3501-6

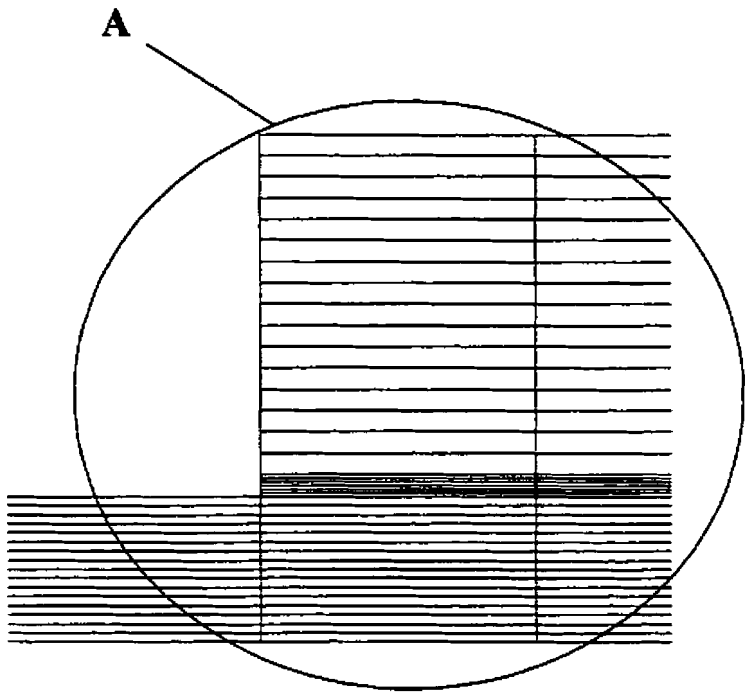

Figure 22: Mesh distribution in region A for the baseline model, element ratio 0.01

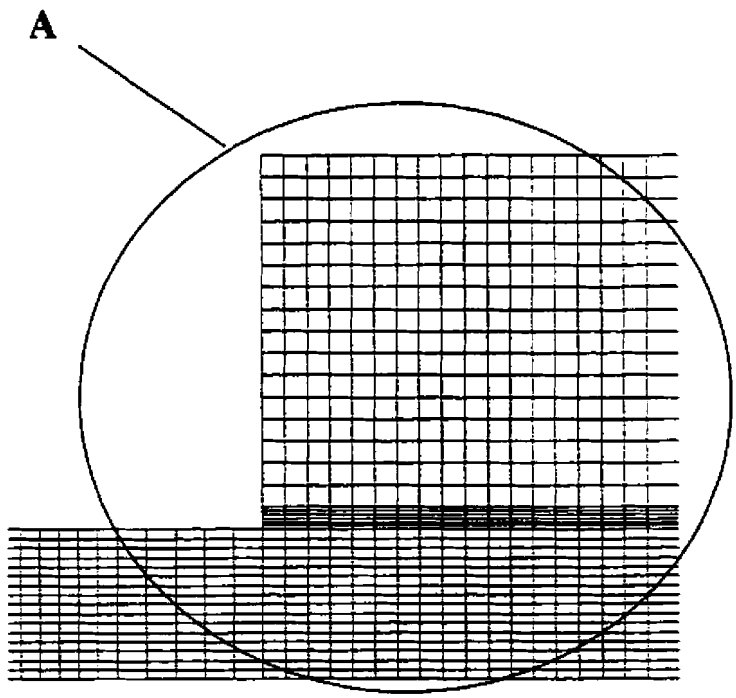

Figure 23: Mesh distribution in region A for baseline model, element ratio 0.25

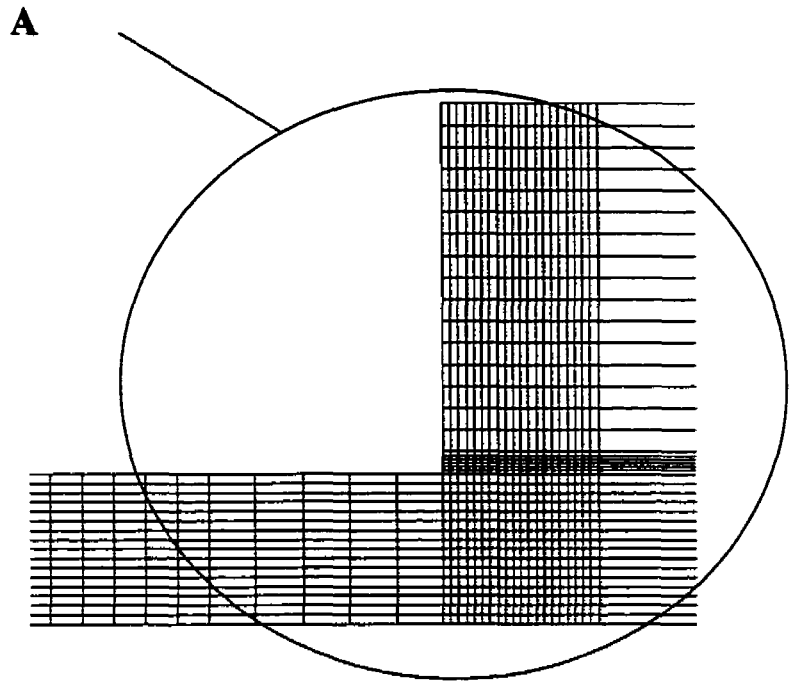

Figure 24: Mesh distribution in region A for the baseline model, element ratio 0.5

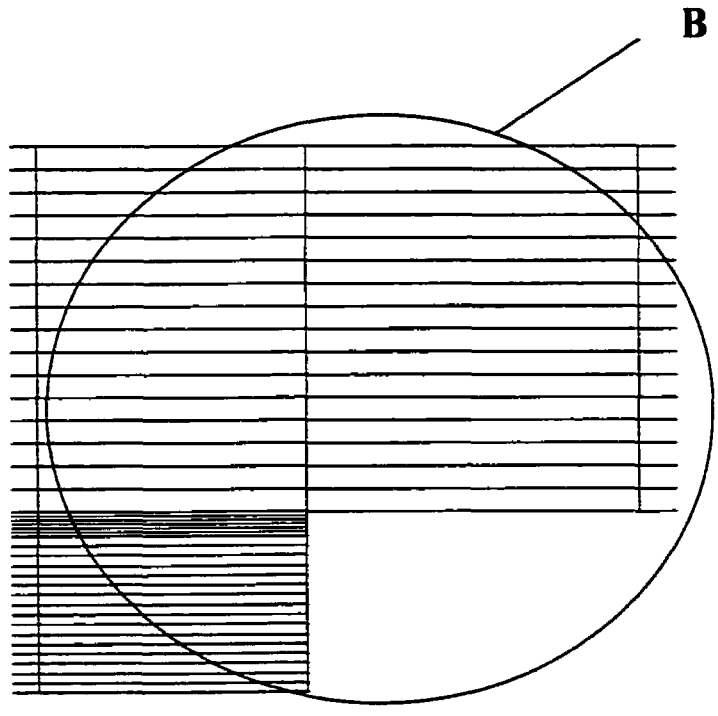

Figure 25: Mesh distribution in region B for baseline model, element ratio 0.01

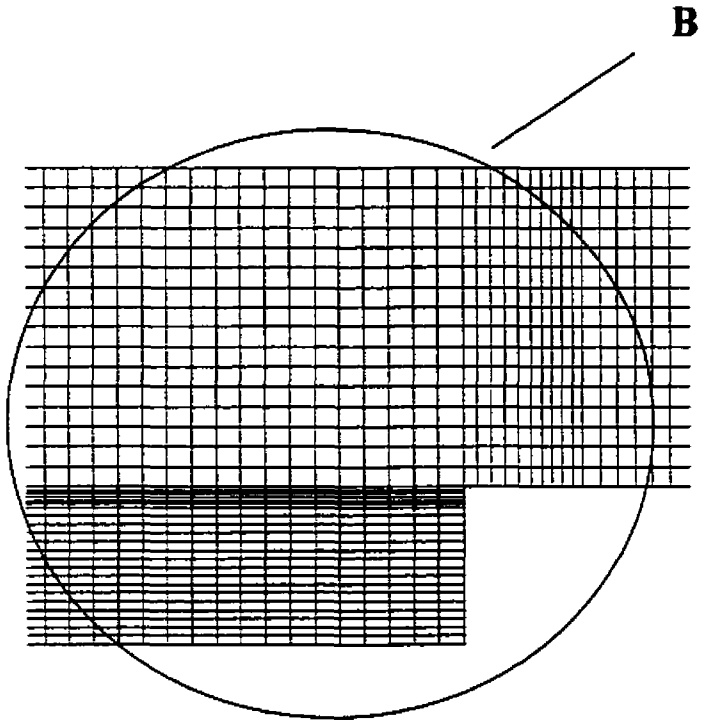

Figure 26: Mesh distribution in region B for baseline model, element ratio 0.25

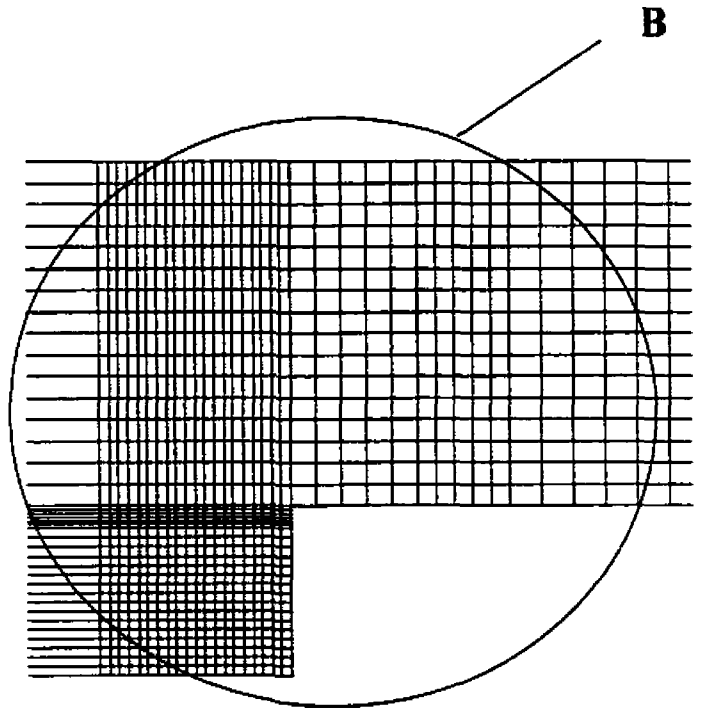

Figure 27: Mesh distribution in region B for baseline model, element ratio 0.5

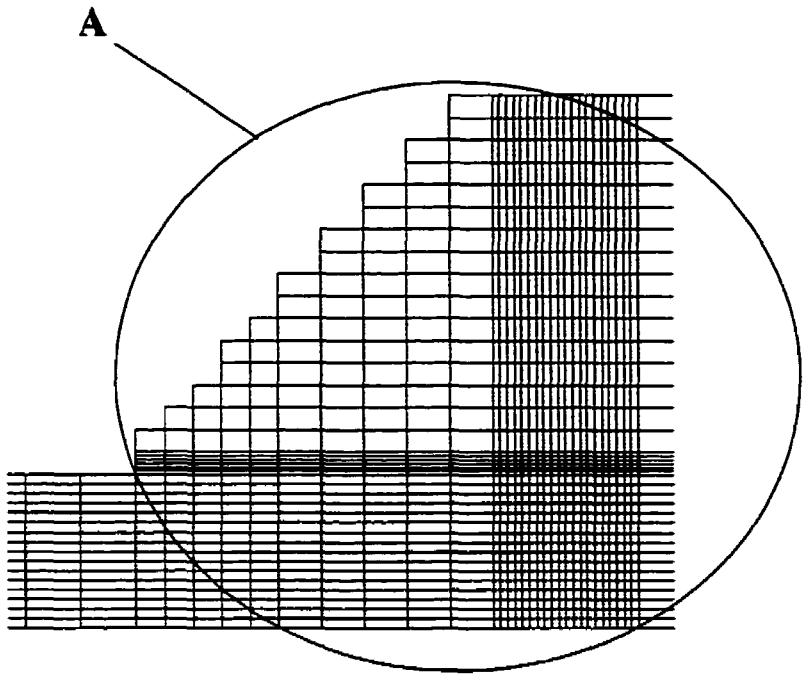

Figure 28: Baseline model with outer bead of 45 degrees, region A

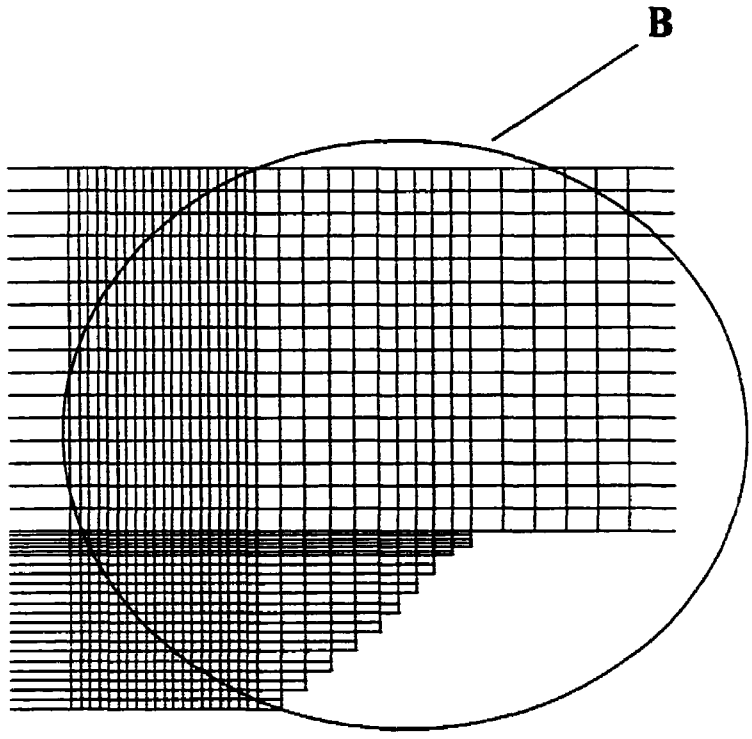

Figure 29: Baseline model with outer bead of 45 degrees, region B

3.2.1 Loading and Boundary Conditions

In the present finite element analysis, the single-lap joint is investigated under two different loading conditions:

(i) Single-lap joint under out-of-plane load (bending)

(ii) Single-lap joint under in-plane load (tension)

In the case of a single-lap joint under out-of-plane load, the applied load in the finite element model is a point load, and the single-lap joint has the boundary conditions of a simply supported beam, Fig. 30. Boundary 1 has restrictions in the x and y directions. Boundary 2 has restriction in the y direction and freedom of movement in x direction.

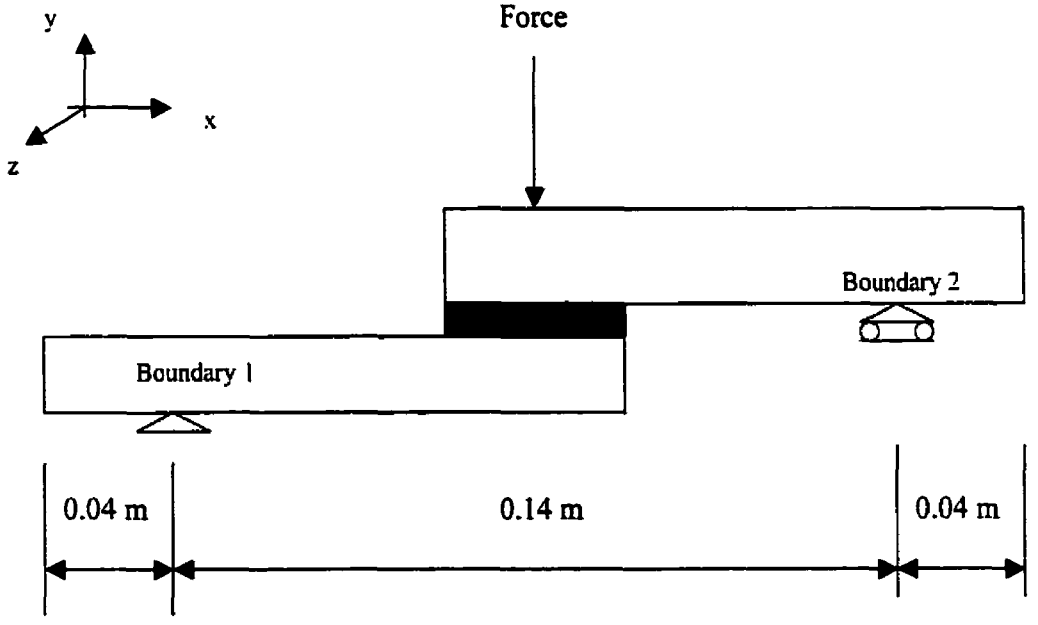

Figure 30: Loading and boundary conditions for a single-lap joint under out-of-plane load

In the case of a single-lap joint under tension, the finite element model is modeled in the way to simulate a tension test, Fig. 31. Rigid elements are used in the place where the in-plane force is applied (Appendix A). Tension force is applied on the composite material

(cross-ply laminate composed of zero and ninety degree layers). For the cases of evenly distributed pressure applied on the elements (without creating rigid surface) or point load, one will obtain nonuniform displacement at the end because of the material property differences in fiber and matrix direction. One will obtain more displacement in the ninety than zero degrees layers. Also both sides of the single-lap joint will be gripped during experimental work (Fig. 36), so that 0.0254 m from each end is taken as grip size and boundary conditions are applied as shown in Fig. 31. Boundary conditions are applied in a way that allows the free rotation of the joint (overlap region is not influenced by boundary conditions).

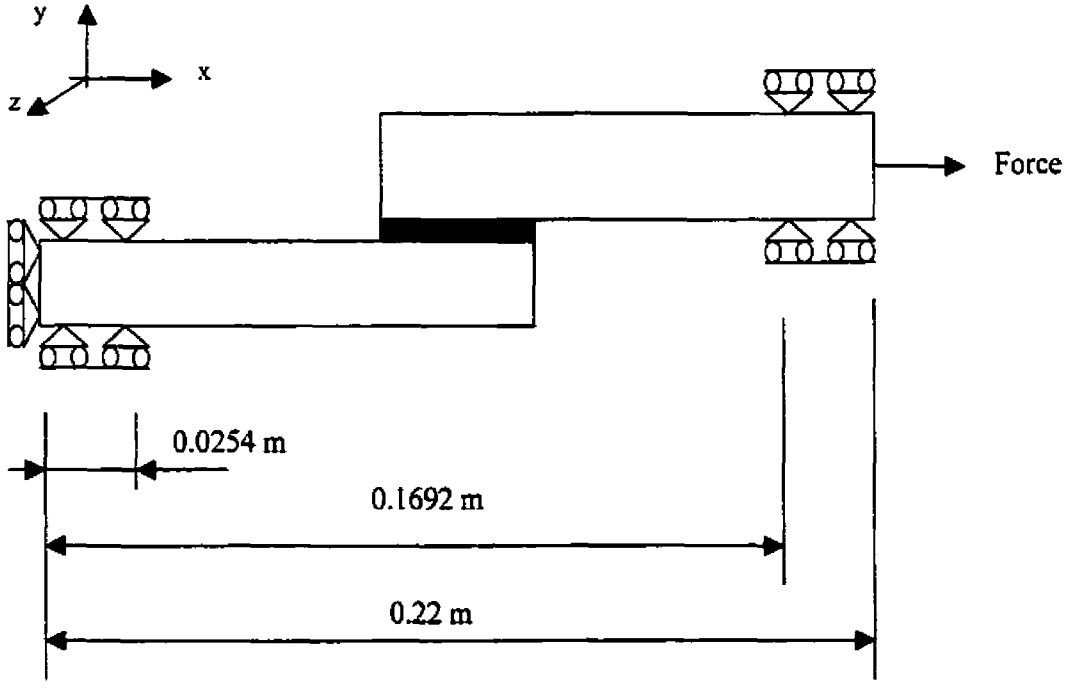

Figure 31: Loading and boundary condition for the single-lap joint under tension

In Fig. 31, there are two different boundary conditions:

Is a boundary condition that has restriction of movement in the y and freedom in the x direction.

Is a boundary condition that has restriction of movement in the x and freedom in the y direction.

Chapter 4

4 EXPERIMENTAL WORK

4.1 SPECIMEN PREPARATION

Adhesive bonding is an intricate process that depends on a number of factors. This is especially true in applications such as those found in the aerospace industry where high performance and durability are critical. One of the main considerations in obtaining a good bonded joint is the effect of surface preparation. In the case of metals, it is common to find a weak oxide layer that in turn may absorb contaminants such as organic molecules or even water. Besides the obvious effect of having a weak oxide layer at a bonded interface, the presence of a layer of contaminants will lower the surface energy thus affecting the process needed to bring the adhesive into intimate contact with the adherend. It is always useful to contact the adhesive producer in order to verify the bonding process that is recommended for the type of the adhesive that one is using.

The adhesive that is used in this research is Depend 330 [33]. In order to join titanium and composite plates to make a single-lap geometry with geometry parameters that are shown in Figs. 17-20 and Tables 1 and 2, Loctite Corporation [33] made instructions for use of their product: For best performance, the bond surface should be free of grease, cleaned by acetone and dried. To ensure a fast and reliable cure, Activator 7387 [33] should be applied to one of the bond surfaces and the adhesive on the other surface. The recommended bond line gap is from 0.1 mm to 0.5 mm, and for gaps of 0.5 mm activator should be applied to both sides. Parts should be assembled immediately. The bond should be held clamped using fixtures, Fig.32. The joint should be allowed to develop full strength before being subjected to any service load, that is, 24 hours after installing in the bonding jig. The jig is pre-sprayed with a release agent, Freekote 770 [34], which prevents the adhesive from curing to the parts that do no belong to the joint configuration.

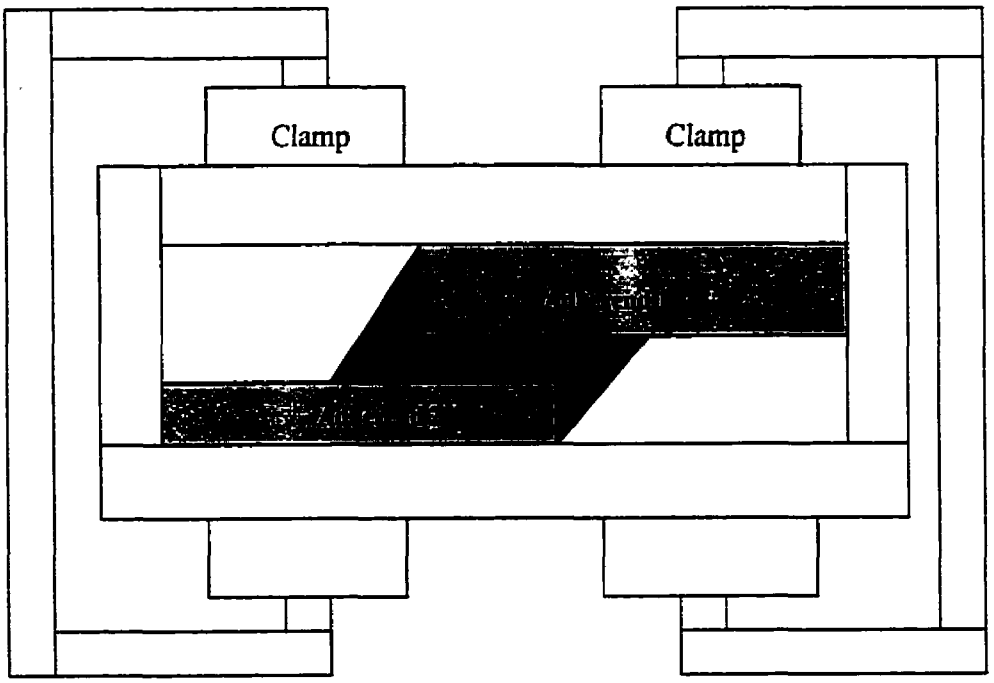

Figure 32: Single-lap joint in a jig

For the present analysis, 60 specimens are made with 5 different geometries, Table 6, according to instructions that are given by the Loctite Corporation. The specimens are tested under two loading conditions: (i) out-of-plane load (bending) and (ii) tension, in order to verify the finite element model and failure analysis of such joints. In the next section, the two loading set-ups will be introduced, Figs. 35 and 36, that are used to evaluate the strength of the single-lap joints and verify the finite element model.

4.2 EXPERIMENTAL SET-UP

4.2.1 Single-Lap Joint under Out-of-Plane Load (Three-Point Bend Test)

The three-point bend test is performed as shown in Fig. 35. The experimental set-up (Fig. 35) and the finite element model (geometry parameters and boundary conditions given in Fig. 30) are modeled to be as similar as possible. Five different sample configurations have been tested with a total of 36 specimens, as shown in Table 6. Failure load, obtained during the experimental work, is also given in Table 6, and full analysis and comparison with finite element analysis is given in the next chapter.

According to the way the load is applied in the three-point bend test, Fig. 35, one will not obtain constant moment in the central section. That can only happen if one does a four-point bend test, Fig. 33. When bonding two different materials with different bending stiffness (1 mm titanium plate and $[0_4/90_4]_s$ cross-ply laminate), the material with lower bending stiffness (titanium) will bend more easily. For large deflections this will not give constant moment in the section, even for the four-point bend test. On the contrary, the loading condition that is obtained this way is going to be close to a three-point bend test with the load that is applied away from joint center, Fig. 34. This occurs because most

of the load will end up on the stiffer portion of the structure, thus the load on the titanium will be small. This is the reason why regular three-point bend test is chosen.

Testing was performed using an MTS machine that has a minimum load cartridge of 25 KN. Since the single-lap joint is more sensitive to out-of-plane than in-plane load, using the load cartridges of 25 KN will cause problems in trying to register a failure load that is only 1 % of the full scale that the machine can register. Therefore, a small load cell is attached to the MTS machine, Fig. 35, in order to be able to register load changes even as low as 1 N. The maximum load that this new load cell can register is 1 KN.

Using a small load cell did not solve all problems, because the load cell could not output displacements, so the displacement had to be read from the MTS machine. When one has to read displacements obtained from a testing machine where all connectors and fixtures are attached by mechanical fasteners to the parent (MTS) machine, error is very likely. In order to be as close as possible to reality, the actual displacement is measured using a dial gauge. As a test, a 60 N load has been set on the machine and the dial gauge is used to measure displacement. At the same time, the displacement cartridge in the MTS machine was recording its own displacement. The recorded displacement from dial gauge was 5.2 mm and from MTS machine, 5.9 mm. The analysis was repeated five times, with different specimens but with the same load and the same specimen geometry.

After tests and comparison, it is found that MTS machine recorded bigger displacements by about 15 % than dial gauge, and therefore the displacements that are obtained from MTS are scaled (decreased) by 15 % henceforth. The registered value for the displacement is essential for the evaluation of the finite element model. The evaluation of the finite element model and results that are obtained from the finite element analysis for joints under out-of-plane and tension load, with comparison to the experimental work done for the same type of joints, is given in Chapter 5.

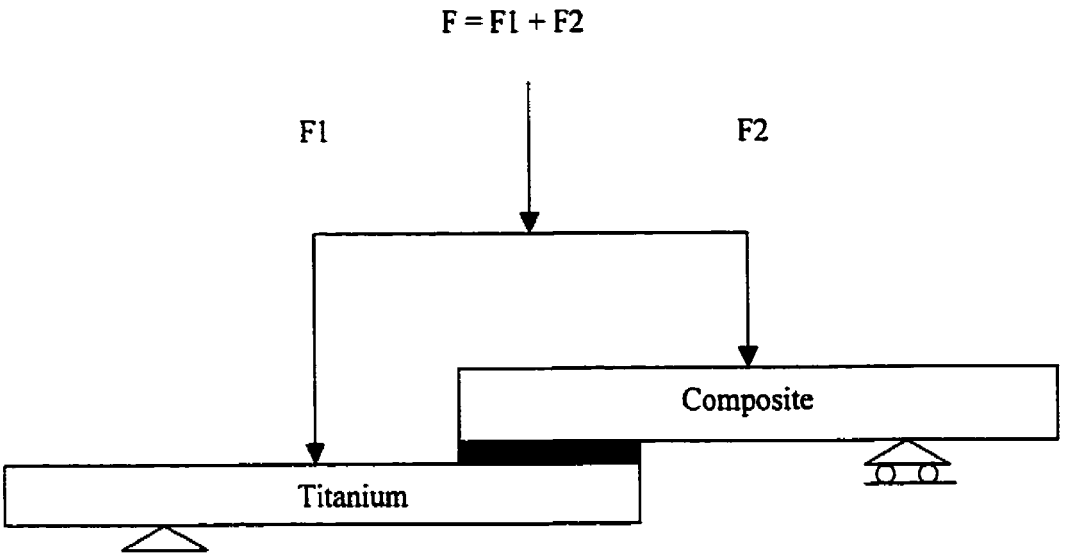

Figure 33: Four-point bend test

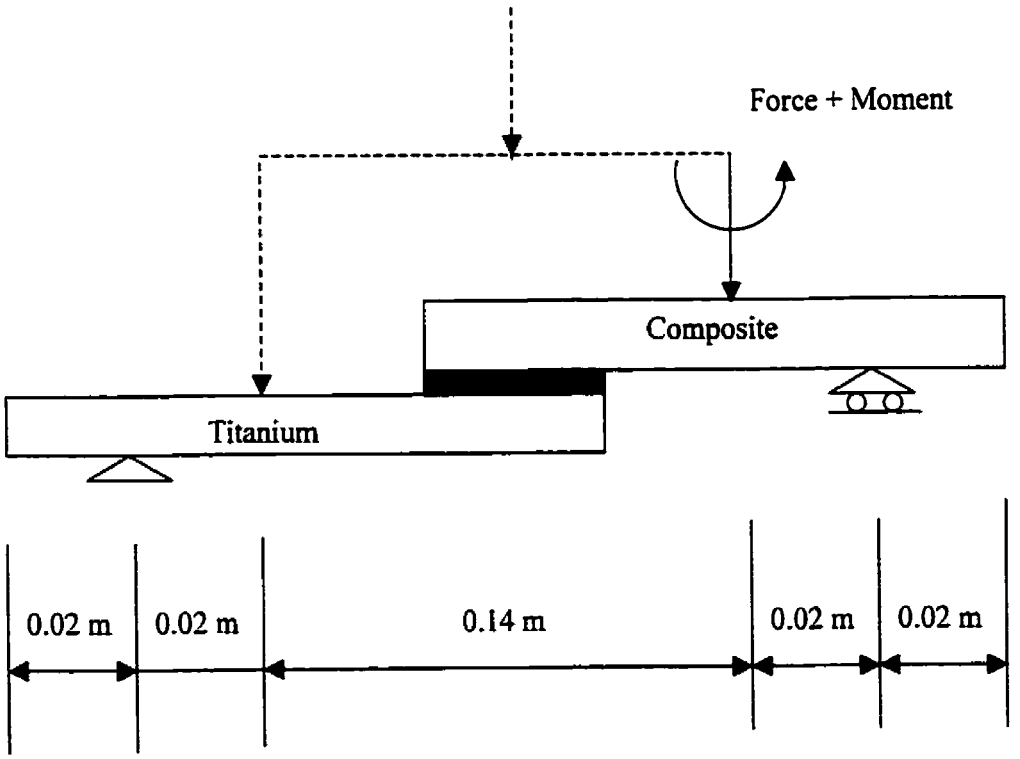

Figure 34: Four-point bend test becomes equivalent to three-point bend test with load applied away from joint center

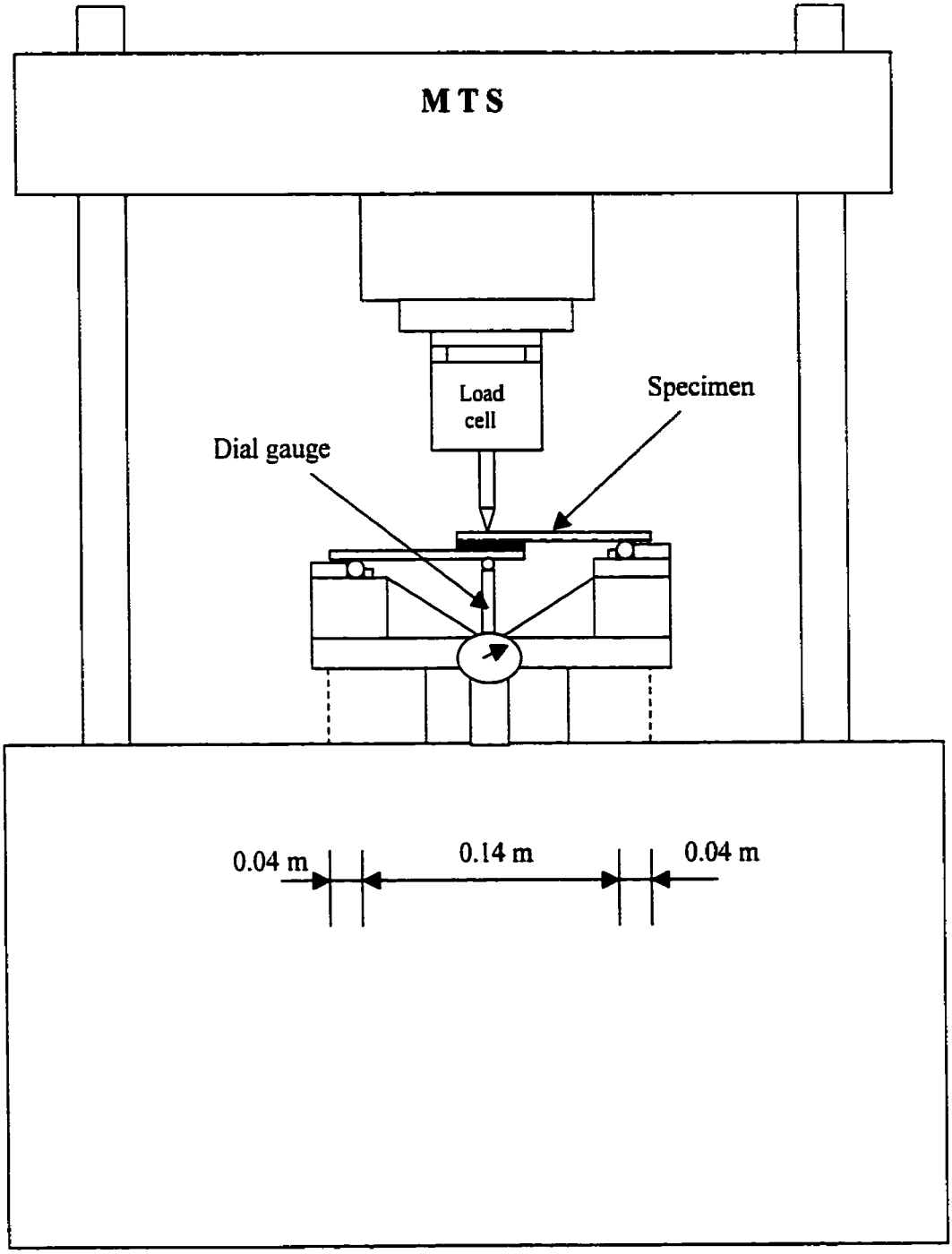

Figure 35: Three-point bend test set up

4.2.2 Single-Lap Joint under In-Plane Load (Tension Test)

For tension tests, 24 specimens with 5 different geometry configurations are tested, according to Fig. 36 and Table 6. As in the bending case, the tension experimental set up (Fig. 36) and finite element model with its parameters (Fig.31) are trying to simulate the same case, where the single-lap joint will be exposed to the in-plane load at the both ends, Fig. 1. It is very important to allow the free rotation of the joint, thus grip the specimen well away from joint center (0.0254 m from each end, both in the finite element model and in experimental work, Figs. 31 and 36).

It is observed that if the upper and lower grips are not centered, it will contribute to additional joint rotation. In order to prevent the extra rotation of an uncentered joint, small inserts have to be placed at each end (where the joint is griped). These inserts enable the joint to be gripped while keeping the specimen perfectly axial and allowing free rotation, Fig. 36.

The tests are performed using a smaller MTS testing machine that has the ability to register an applied load of up to 10 KN. Since the single-lap joint is designed in a way that can accept more in-plane than out-of-plane load, expected failure load for the specimen is around 40 % of the full scale of the load cartridge (10 KN) so there was no need to install the small load cell. The results obtained from this experimental set up are presented in Table 6, and comparisons with finite element results are given in Chapter 5.

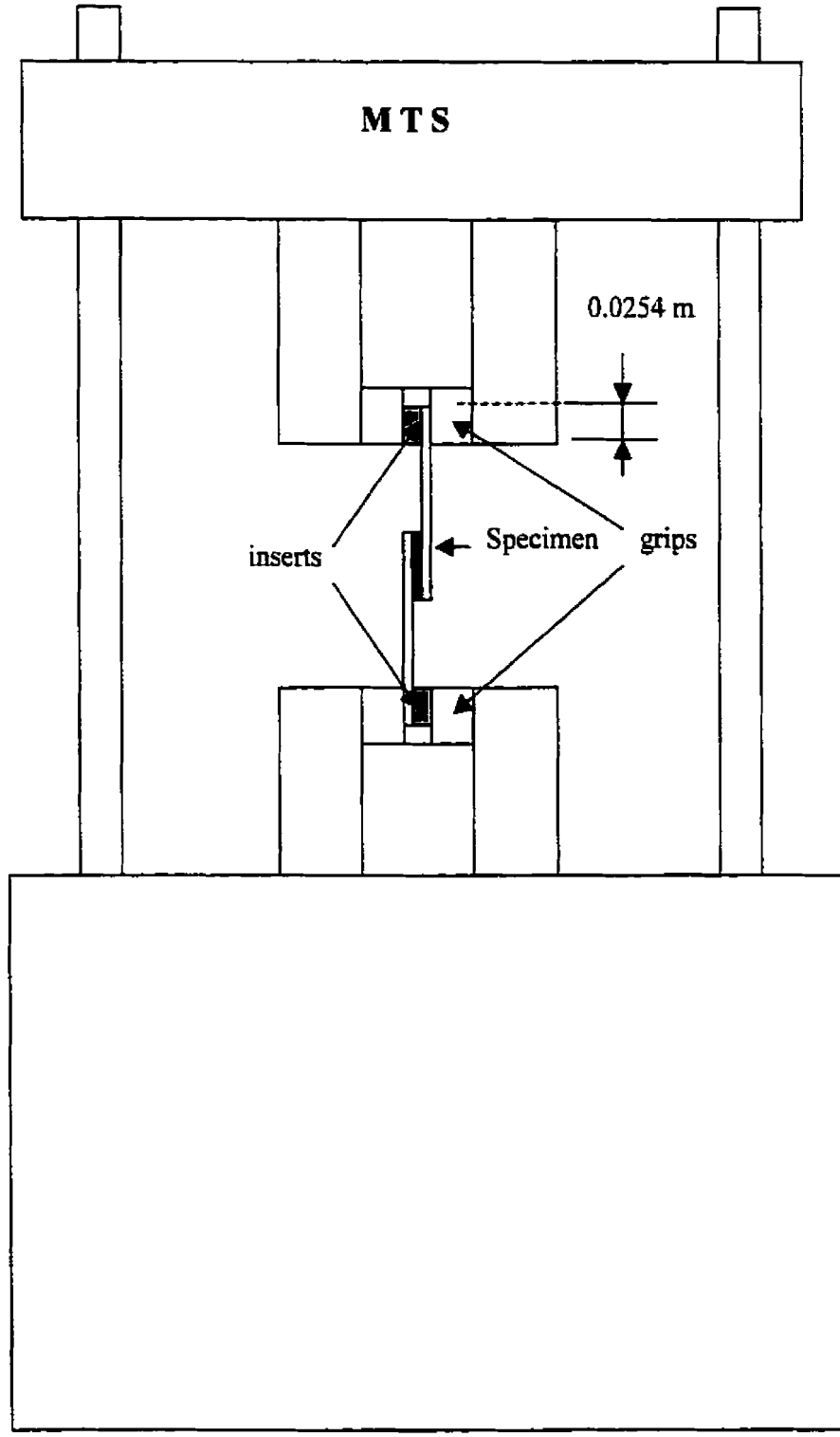

Figure 36: Testing set up for a single-lap joint under tension load

TEST	Quantity		Taper angle	Av. Failure Load (N)	
	No outer bead, +α	With outer bead (45°), +α		No outer bead, +α (Sta. Dev.)	With outer bead (45°), +α (Sta. Dev.)
Bending	5	3	α =0°	109 (0.7)	182 (2.6)
Tension	3	3		3820 (116)	4526 (87)
Bending	5	3	α =1.43°	119 (1.4)	230 (1.0)
Tension	3	3		3830 (112)	4835 (110)
Bending	5	3	α =2.04°	120 (1.5)	212 (1.2)
Tension	3	3		3900 (105)	4817 (125)
Bending	5	3	α =3.57°	119 (2.3)	212 (2.0)
Tension	3	3		3880 (101)	4825 (98)
TEST	**Quantity**		**Taper angle**	**Av. Failure Load (N)**	
Bending	4		β=1.43°	108.5 N (1.3)	

Table 6 : Experimental results for three-point bend and tension test

Chapter 5

5 RESULTS

5.1 FINITE ELEMENT MODEL AND DESIGN VERIFICATION

Chapter 4 introduced the way that displacements of the single-lap joint under out-of-plane load were recorded (displacements that were recorded by the displacement cartridge decreased by 15 %, according to a calibration by a dial gauge). One of the ways to verify the finite element model with the physical model is to compare displacements of both models that were obtained for the same loading condition.

ABAQUS [32] finite element code has an option to output a Displacement vs. Load curve for nodes of interest. The displacements and forces applied in the ABAQUS finite element code are given with respect to time (quasi-static analysis). Also, the displacements and applied load from testing machine were recorded respect to time, with the final comparison of those values given in Fig. 37. In Fig. 37 displacements, ABAQUS and Experimental, have been obtained for an applied force that increases in

time from 0 to 109 N. From Fig. 37, one can see that finite element results are very close to the ones obtained from experiments. For the final level of the force (109 N), the displacements obtained were: (i) 8.9 from ABAQUS, and (ii) 9.3 mm from experiments. At this point, there is a good indication that finite element simulation corresponds to physical model.

Design recommendations for single-lap joints that have been accepted from literature are:

- Overlap length of at least 20 mm, Ref. [26]
- Bondline thickness of 0.15 mm, Ref. [3]
- Inner tapering and adhesive fillet (45 degrees) is a highly efficient technique for reducing stress peaks both in the adherend and in the adhesive and hence in improving joint strength, Ref.[2, 3 and 13].
- Outer tapering is used to improve load transfer in the structure, and in this way the stress concentrations are minimized and the joint strength is improved, Ref. [2].

It has not been shown that for joining a titanium plate 0.12 m x 0.0254 m x 0.0001 m with a composite cross-ply laminate $[0_4/90_4]_s$, an overlap length of 0.02 m will provide full efficiency of the joint. The Ref. [26] also states that as one increases the overlap length the adhesive shear stress is reduced. However, it is evident that beyond a certain overlap length, one reaches point of diminishing returns. In Fig. 38, a much greater reduction in the peak of the shear stress distribution occurs for overlap changes from 0.01 m to 0.02 m than from 0.02 m to 0.03 m. The Ref. [3] states that the optimum bond thickness is between 0.12 and 0.25 mm, and that larger thickness will tend to decrease stiffness of the adhesive. In this way, this design recommendation (overlap length) for the single-lap joint Fig. 17 is verified and the analysis is continued towards the optimization of the exposed ends of the single-lap joints subjected to in-plane and out-of-plane load. The second design recommendation that was accepted is verified in the next section that talks about strength prediction of adhesivly bonded joints (5.2).

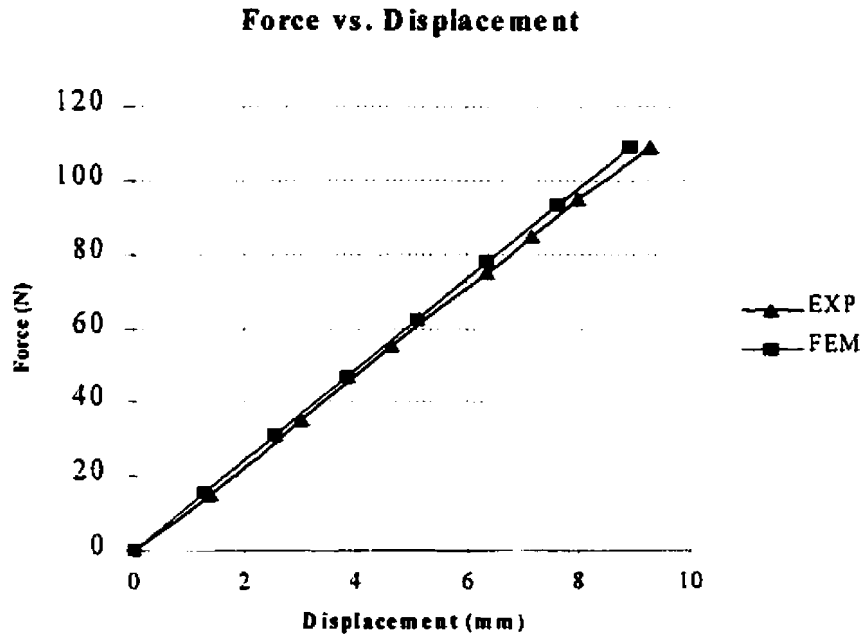

Figure 37: Force vs. Displacement curve for a baseline model subjected to out-of-plane load

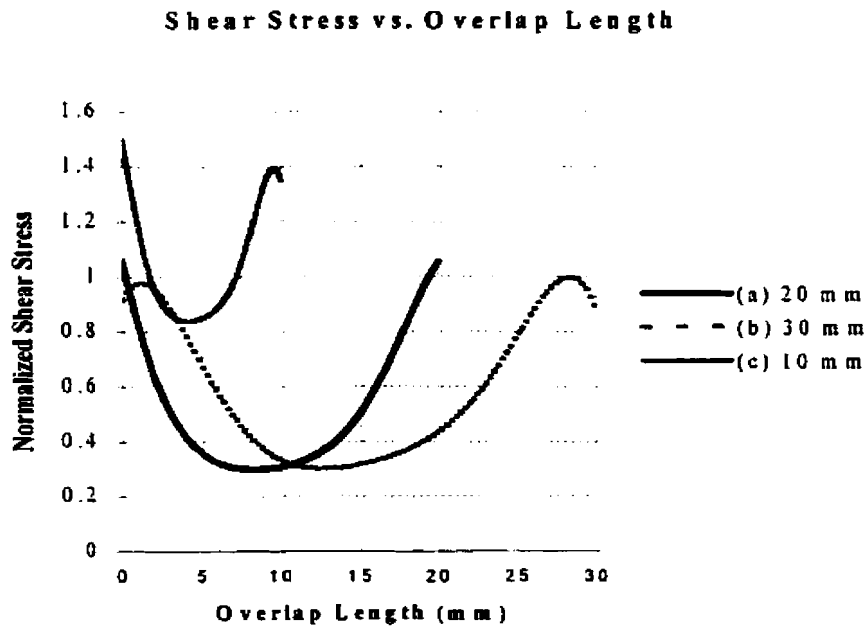

Figure 38: Shear stress distribution in titanium-composite interface region

(Shear stress normalized with respect to shear strength)

5.2 STRENGTH PREDICTION FOR SINGLE-LAP JOINTS BY STRAIN ENERGY METHOD

In Chapter 2, it was shown that for any stress-based failure criteria used to predict the strength of adhesively bonded joints, if failure occurs in the adhesive, there will be mesh density problems. In Figs. 7 – 15, it was shown that the main stress components in the adhesive at the vertex, for different element ratios, drastically change in value with mesh refinement. On the other hand, in Chapter 2, the strain energy obtained as an output from the element stresses in the adhesive (overlap region) did not vary at all for element ratios of 0.025 and 0.5, Fig.16. The strain energy at failure converged.

The stress singularity problem was solved, but it was impossible to predict joint strength only by the finite element model since the strain energy value depends on the joint geometry. Therefore, the first step was to indicate the validity of finite element model with a force vs. displacement curve (Fig. 37), and then find failure load for the baseline model experimentally (Table 6). In the second step, this load was used in finite element model. As one can notice, the failure load for baseline model was not determined by FEA. It was determined by experiment. Reference value for strain energy was not determined by experiment. It was determined by FEA.

From experimental work, Table 6, it was determined that average failure load at which a single-lap joint (without any taper) failed (baseline model) was 109 N.

ABAQUS finite element code can output strain energy for elements that represent only overlap adhesive and the result was 1.012 E-2 J of strain energy. The value is calculated for all elements that represent adhesive, and this value is obtained for one geometry and one load (baseline model at 109 N load). Obviously, this value changes when one changes the load and keeps the same geometry of the joint. ABAQUS finite element code calculates strain energy by the method shown in the equations 5.1 – 5.11.

The stress-strain state in the region of interest (overlap of the adhesive) will determine the value of the strain energy. The value that is obtained for the baseline model subjected to 109 N of out-of-plane load is henceforth accepted as a reference value (1.012 E-2 J). Fig. 39 shows the method for predicting failure load for the single-lap joint that has a different geometry, e.g., an inner taper of α = 1.43 degrees. Finite element failure load is predicted to be the load that brings the overlap adhesive (the same region as one that belonging to the baseline model, Fig. 17) into a stress-strain state of similar strain energy to that brought about by the out-of-plane failure load (109 N). One point on the graph (0, 0) Fig. 39, is always known, because if there are no forces on the boundary of the structure, there is no work done. One need to take at least two arbitrary loads and use them as input in the finite element model to determine two more strain energies of the adhesive. Through those three points a parabolic curve can be drawn similar to that shown in Fig. 39. The y-axis represents the strain energy distribution in the adhesive, and the x-axis represents the applied load.

Drawing a horizontal line from the baseline strain energy value of 1.012 E-2 J, and going to the intersection with the curve that passes through the three points yields the x-axis value of the load that brings the single-lap joint with inner taper of 1.43 degrees to failure. The value of this load is about 116 N. This means that a load of 116 N will fail a single-lap joint with inner taper of 1.43 degrees in the same way that out-of-plane load of 109 N failed the baseline model. One can notice an improvement in the joint design of 7 N, which means that the applied load has to be larger by 7 N than the baseline load (109 N) in order to fail the joint with inner taper of 1.43 degrees.

For the joints under tension, the same approach is used as above, but now the joint strength in tension is predicted from a bending strain energy analysis. It is expected that a much larger in-plane load is required to bring the overlap adhesive into the similar stress-strain state than that brought about by the out-of-plane failure load (109 N), since the single-lap joint is more sensitive to out-of-plane than in-plane load. For the tension case, Fig. 40, the (0, 0) position is known, and one has to chose at least two more arbitrary loads in order to determine the strain energy in the adhesive (by finite element

method) and draw the curve through three points, Fig. 40. This curve represents the strain energy in the adhesive (y-axis) that is obtained from applied load (x-axis).

For 1.012 E-2 J of strain energy, the intersection with the curve that is drawn through three points corresponds to 3650 N load on the x-axis (Fig. 40). This means that one needs to apply 3.65 KN of in-plane load (tension) in order to bring baseline tension model into a similar stress-strain state to that brought about by an out-of-plane force of 109 N.

In Fig. 41, the strength prediction for a single-lap joint with different bondline thickness is evaluated by the strain energy method. Notice that the predicted strength decreases with increasing thickness of the adhesive. For adhesive thickness of 0.05 mm and 0.15 mm the predicted strength is almost the same.

During the manufacturing process, it is very important to achieve the desired adhesive thickness and reduce production time. In order to provide a bondline thickness of 0.05 mm and lower, a very high clamping force has to be applied on the bonding jig. There is also a problem with taking a specimen out of the jig even if release agent is applied, Fig 31. During the manufacturing process, adhesive will overflow on each side of the jig and will cure all components of the jig together. The bondline thickness is ensured by a small plate that goes between the composite and titanium adherend. When disassembling the cured specimen from the jig, the very thin plate that is providing the bondline thickness can be damaged easily and its dimensions change. Bondline thickness cannot easily be kept at 0.05 mm. The result is usually a variable bondline thickness in the range 0.05 to 0.15 mm.

An adhesive thickness of 0.15 mm is accepted as a good bondline thickness for the model that is introduced in this research. The rest of joint geometries (Figs. 18, 19, and 20, with Tables 1 and 2, for tension and bending load) are analyzed in the same way as above (Figs. 39 and 40) and results of these analyses are used to find the optimum design of the single-lap joint geometry.

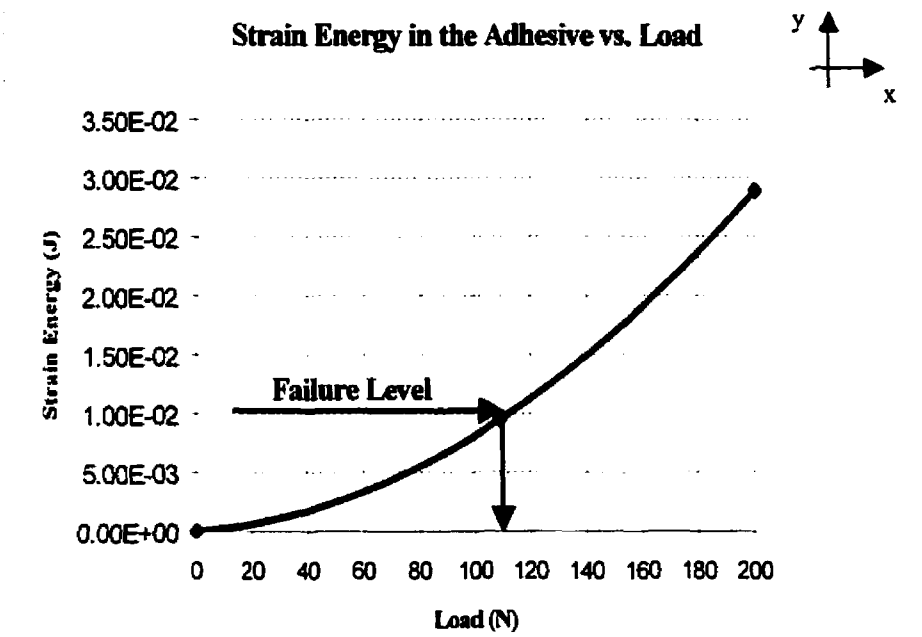

Figure 39: Strain energy in the overlap adhesive for baseline model in bending

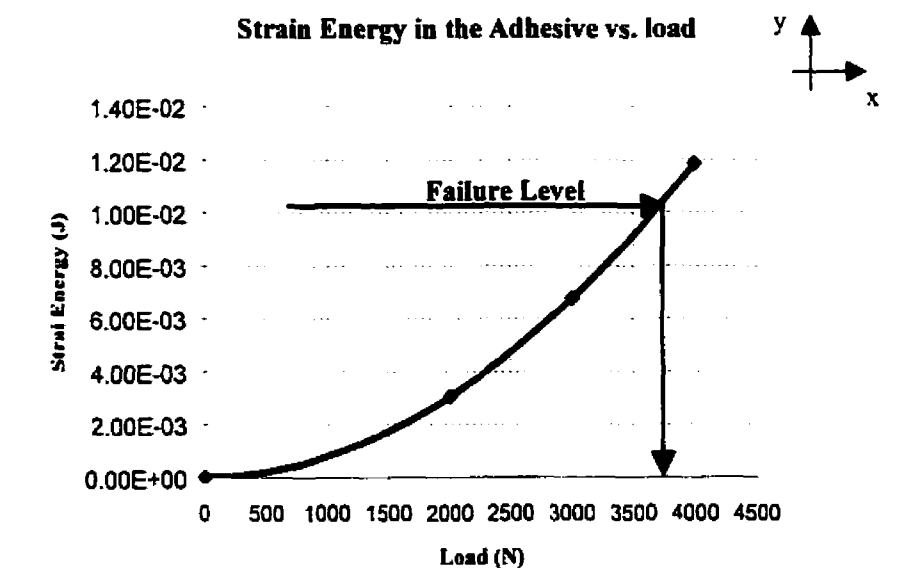

Figure 40: Strain energy in the overlap adhesive for baseline model in tension

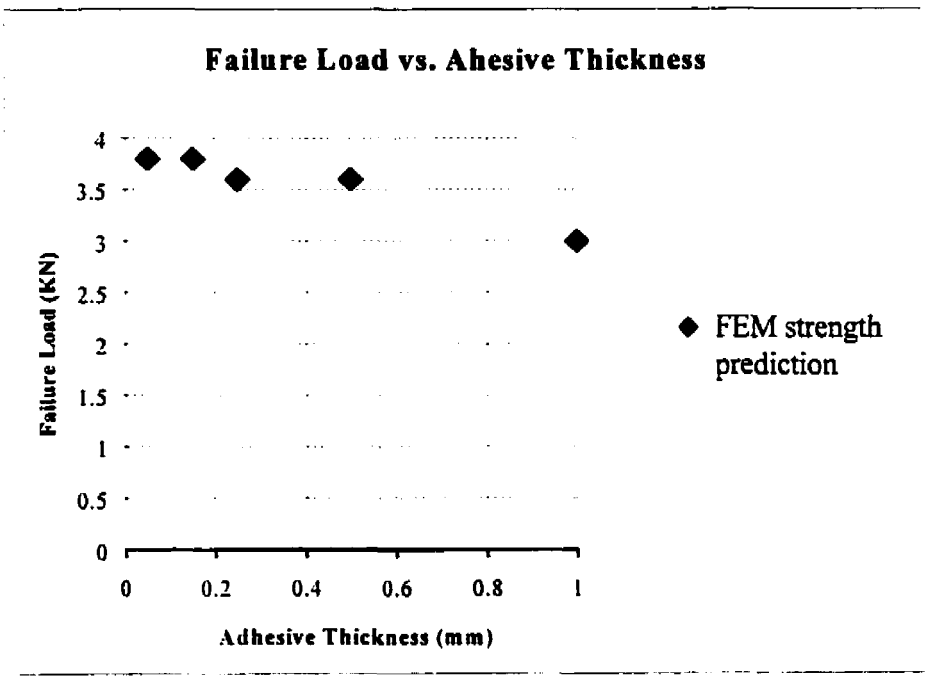

Figure 41: Tension failure load for a single-lap joint with different adhesive thickness

5.3 OPTIMIZATION

5.3.1 Single-Lap Joint under Out-of-Plane Load

In order to find the optimum design of the single-lap joint, the strength values that are obtained from the finite element analysis and the experimental work are plotted versus the joint geometry, Figs. 42 - 45. In each of the finite element simulations, four points are used to generate the curve. In order to create one curve, 10 - 12 simulations had to be performed with methodology for strength prediction shown in Figs. 39 and 40. The finite element strength values for the single-lap joints, with geometry that is shown in Figs. 18, 19, and 20, were determined by the strain energy method, and experimental results are

used from Table 6. As shown in Table 6, the baseline model failed under 109 N of out-of-plane load, and in Fig. 42, which is used as a reference load. For the cases of inner taper under bending loads (Fig. 42), when the design variable b varies from 0.5 mm to 0.9 mm there is an increase in the joint strength. The peak value for the bending case (around 120.5 N) is obtained for design variable b= 0.9 mm and inner taper $\alpha = 4 - 5$ degrees. For b= 0.5 mm, the peak value is about 117 N for FEM and about 120 N for experiments with inner taper of about 2 degrees. For design variable b=0.75 mm and the inner taper between 3 and 4 degrees, the highest strength value is about 120 N. Notice that there is no significant strength improvement obtained for the different design variables: b= 0.5 mm, 0.75 mm and 0.9 mm.

The effect of some outer taper under bending load, on the contrary, can have a negative influence on the joint strength. The outer tapers for angle (β) between 0 and 3 degrees decrease the joint strength, but from 3 to 6 degrees there is strength improvement compared to the baseline model. From Fig. 42 one can see that the experimental results obtained for the geometry b= 0.5 mm (Table 6) and joints strength predicted by finite element model (b= 0.5 mm) correlate well. The strength improvement for the case of outer taper is apparently smaller than the joint strength achieved by inner taper, therefore, further analysis (bending case) is concentrated on the inner taper.

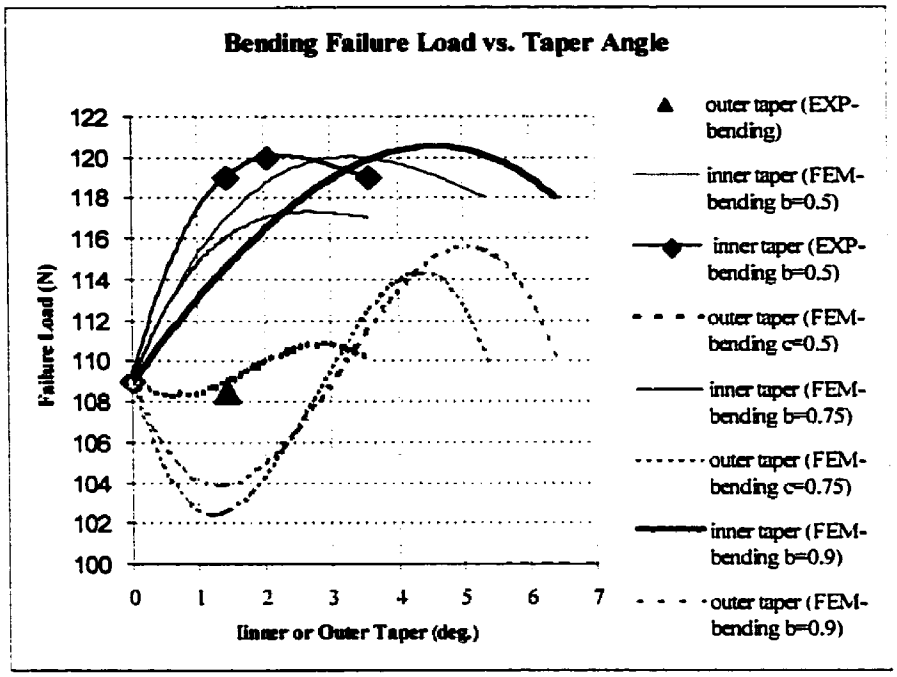

Figure 42: Bending failure load for joints with inner or outer taper

Fig. 43 shows the analysis of single-lap joints with inner tapers and outer epoxy beads. The joints are examined by the finite element method and experimentally. The 45 degree adhesive beads are created in the finite element models as shown in Figs. 28 and 29, and tested samples are bonded in the jig shown in Fig. 32. From Fig. 43, notice that there is a big improvement in the joint strength for the single-lap joints that have inner taper and outer beads compared to the baseline model. In this analysis, good agreement is found between the experimental and finite element results. The maximum strength (about 249 N) is obtained for the geometry variable b= 0.9 mm, and angle of inner taper (α) of about 2 degrees. For b= 0.5 mm and inner taper angle of about 1 degree, the strength of the adhesive joint is about 219 N for the FEM and about 233 N for the experiment. The single-lap joint with design variable b= 0.75 mm and 2 degrees of inner taper failed at maximum average load of about 233 N according to the FEA, Fig. 42. For the case where the single-lap joints were subjected to the out-of-plane load, the inner taper of 2 degrees from design variable b=0.9 mm in combination with an epoxy bead of 45 degrees

gave the best strength result. This case is thus an optimum design for a single-lap joint under bending load, and the optimum design for the single-lap joint under in-plane load (tension) is discussed in the next section.

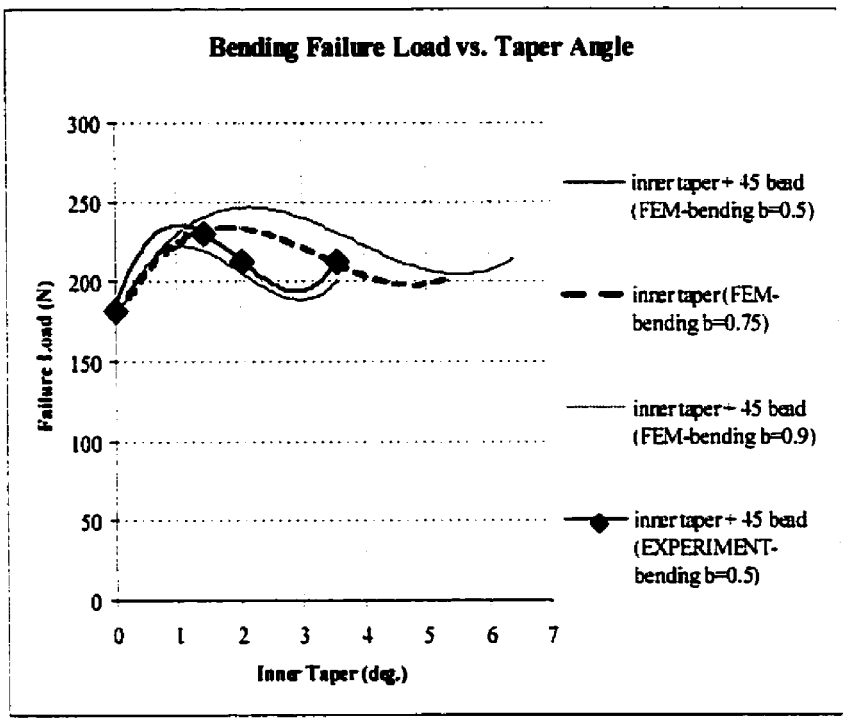

Figure 43: Bending failure load for joints with inner taper and outer bead

5.3.2 Single-Lap Joint under Tension Load

For the case of tension (Fig. 44), with a range of the design variable b from 0.5 mm to 0.9 mm, there is no increase in the obtained strength values. Notice that inner taper in tension produced the same effects as outer tapers in the bending case. In the region α= 0 - 3 degrees there is a decrease in the joint strength, but from α=3 - 6 degrees, the joint strength improved. Also, for the bending case (without outer bead) the peak value was

obtained for design variable b= 0.9 mm (about 120.5 N), but in the tension case the optimum value was obtained for b= 0.5 mm (about 3.9 KN for FEM and experiment). In Fig. 44 it is possible to see good agreement between finite element analysis and experimental results that are obtained for design variable b= 0.5 mm (thick black line and thick gray line). The outer taper gives a small increment in strength with increase of the design variable c (0.5, 0.75, 0.9 mm). This does not happened in the bending case, where the outer taper produces a negative effect on the joint strength.

Also, as was the case for bending, the higher strength values are obtained for inner rather than for outer tapers. Epoxy beads are not very practical for the joint that has outer taper. Therefore, epoxy beads should be made in combination with an inner taper, as in the previous case. The same approach is then taken as in the bending case, with the outer epoxy bead built on both sides of the joint ends, Figs. 28 and 29. In Fig. 45, it can be seen that epoxy beads did not effect the tension joint strength as much as in the bending case. The peak value is obtained for design variable b= 0.5 mm and inner taper (α) between 1 and 2 degrees (around 4.65 KN for FEM and about 4.8 KN by experiment). The experimental and finite element joint strengths (b=0.5 mm) are in good agreement. Fig. 45. At this point, the optimum design in the tension case is considered to be determined, and design variables have the values: b= 0.5 mm and α =1-2 degrees.

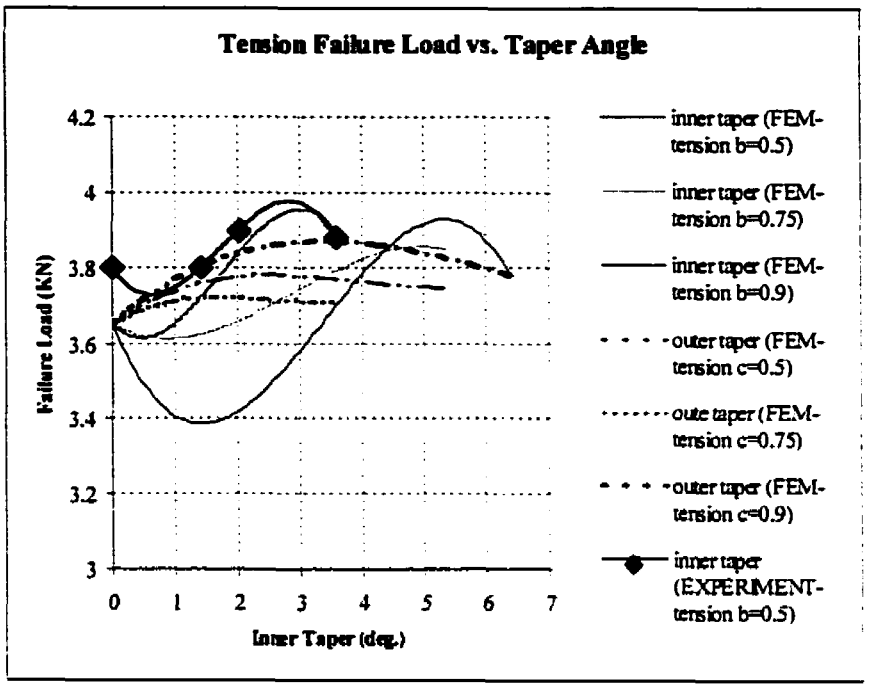

Figure 44: Tension failure load for joints with inner or outer taper

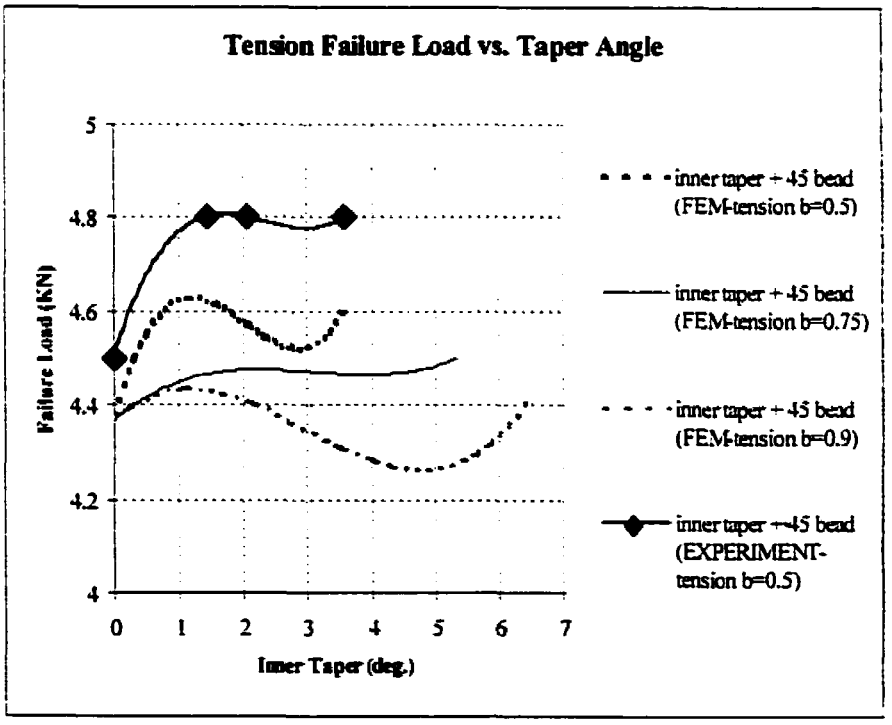

Figure 45: Tension failure load for joints with inner taper and outer bead of 45 deg

5.3.3 Optimum Design of the Joint Ends

From the analysis presented in sections 5.3.1 and 5.3.2, there are two different design solutions that are most suitable for the single-lap joint that is subjected to different loading conditions: (i) bending and (ii) tension. However, the objective in this research is to find the design that is going to suit both loading conditions. For design variable b= 0.9 mm, the single-lap joint achieved the highest strength value in bending. In tension the single-lap joint had the lowest strength for this type of the design (b= 0.9 mm), and the best result was achieved by design variable b= 0.5 mm. In Figs. 42 - 45, notice that results obtained for design variable b= 0.75 mm are in-between the results that are obtained for b= 0.5 and b= 0.9 mm.

If one wants to design the single-lap joint that is going to operate under two different loading conditions, the design variable b= 0.75 mm with inner taper of about 2 degrees and outer bead of 45 degrees will be the most suitable one. Therefore, for the single-lap joint that is subjected to two different loading conditions that are applied alternatively: (i) out-of-plane (bending) and (ii) in-plane load (tension), the optimum configuration at joint ends can be predicted as:

(i) b= 0.75 mm, and

(ii) $\alpha = 2^0 + 2 \times 45^0$ outer epoxy beads (Fig. 46)

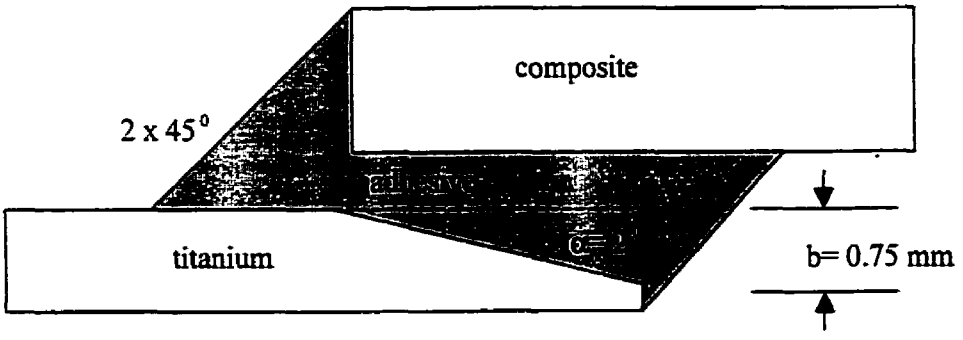

Figure 46: Optimum design for the single-lap joint ends

5.3.4 Summary of the Results of Optimization

The objective of this research was to find the design of the joint ends of single-lap joints between composite material and titanium in order to increase the joint strength.

To join the titanium (0.12 m x 0.0254 m x 0.001m) and the composite plate $[0_4/90_4]_s$ with 0.146 mm ply thickness to form a single-lap joint configuration, the bonding recommendations were accepted from Ref. [2. 3, 13 and 26] and verified:

- Overlap length of 20 mm
- Bondline thickness of 0.15 mm
- Inner tapering of the adherend with adhesive fillet of 45 degrees
- Outer tapering without adhesive fillet

The present analysis verified, accepted and gave new recommendations for the design of the single-lap joint subjected to two different loading conditions: (i) bending and (ii) tension. The present analysis found that:

- Overlap length of 20 mm will provide full efficiency of the single-lap joint.
- An optimum adhesive thickness (bondline thickness) is between 0.05 - 0.15 mm.
- Single-lap joint with inner taper of about 2 degrees and two outer epoxy beads of 45 degrees gave strength improvement in tension (about 23 %) and bending (about 114%).
- Outer tapers did not significantly improve the failure strength in tension or bending.

Chapter 6

6 CONCLUSION AND RECOMMENDATIONS

6.1 CONCLUSION

In this research, optimization of the configuration of a single lap joint is examined. Several design parameters that can govern design of the adhesively bonded joints are investigated: (i) inner tapers, (ii) outer tapers, and (iii) inner tapers in combination with outer epoxy beads of 45 degrees. The finite element models are created using ABAQUS finite element code. The strain energy criteria is used as failure criteria because it converged with mesh refinement and is not effected by stress singularities that exist at the vertices. This criteria can be used for different joint configurations since it is property of the adhesive. For instance, if one has a single-lap joint with overlap length of 1 m, then one should:

(i) Create a finite element model (single-lap joint) with 1 m overlap length .

(ii) Verify the finite element model (force vs. displacement curve can give an indication whether finite element model is good or not).

(iii) Test baseline model and determine failure load (this load will be input load for the finite element model).

(iv) Obtain the finite element strain energy value for the baseline model (overlap adhesive) and accept this value as a reference value.

(v) Use methods shown in Figs. 39 and 40 for strength prediction for configurations different than the baseline model.

In the present analysis, experimental work is performed for two different loading conditions: (i) bending and (ii) tension.

Initially, the four-point bend test is attempted, but differences in bending stiffness between the titanium plate and the composite laminate prevented the experiment from succeeding. Therefore, a three-point bend test set-up is used and 36 samples are subsequently tested.

For tension case, the tested samples have to be centered with the grips so additional inserts have to be implemented in order to prevent additional joint rotation that can lead to earlier failure. For the tension case, 24 samples are tested. In both cases, bending and tension, there is a good agreement between finite element and experimental results. At the end the optimum design of the joint ends is predicted with its design variables.

The best joint design gives strength of (i) about 233 N for the bending case and (ii) about 4.5 KN for the tension case. The baseline model failed at about 109 N for the bending and about 3.65 KN for the tension case. Thus, the improvements for the best design measured from baseline values are: about 114 % for the bending case and about 23 % for the tension case.

From the above results, the finite element analysis method is a good tool for designing and predicting the single-lap bonded joint strength of composite / titanium combinations.

6.2 RECOMMENDATIONS

In the present analysis, the single-lap joint was exposed to the static load and the adhesive was modeled with elastic material properties. Future analysis could implement non-linear material properties for the adhesive and also the dynamic analysis could be performed. Hence, one could see the influence of the design variables that were determined in this analysis and their effect on the joint strength for the single-lap joint under dynamic loading conditions. There is also possibility to extend this work into the area of bolted-bonded joints. The titanium plate could be joined to composite laminate with both adhesive bonding and mechanical fasteners. In this case, one should include the metallic insert in the design and attempt to prevent damage of the hole made in the composite laminate. This bonded-bolted joint also could be examined under two different loading conditions, bending and tension.

As a first step, one could examine the difference in the strength that is brought about by including a mechanical fastener into the structure. Once again, there could be a problem to apply a three-point bending test, because the mechanical fastener is located near mid-span. Therefore, one should attempt a four-point bend test, but first the bending stiffness of the both adherends should be close. If the analysis of the adhesively bonded joints if performed on ABAQUS finite element code, there is also possibility to control input files from the main system such as UNIX. It means that any character in the file can be called with SUBROUTINE and can be replaced with any new character. For instance, if one wants to do elastic analysis of simple plate under tension load, and wants to find out what is minimum thickness of the plate that can stand the applied load. One could:

(i) Create ABAQUS input file

(ii) Perform finite element analysis and obtain stresses and strains.

(iii) Read ABAQUS output (data) file with SUBROUTINE (FORTRAN, C or C++) and find out if the failure analysis is satisfied. If there is no stress that is bigger than Yield stress the dimensions of the plate can be decreased. If the stress is greater than Yield stress the dimensions of the plate have to be increased in order to withstand applied load.

(iv) Change the coordinates of the nodes by SUBROUTINE.

(v) Repeat finite element analysis until the minimum thickness for the plate is found.

Notice that there are several SUBROUTINES that operate at the same time, but all those SUBROUTINES can be linked by shell script programming in one file. Therefore, there is a possibility for changing geometry variables that govern design instead of placing those variables as constants into ABAQUS input file. There is also a possibility to change material and element properties, but in that case one has to create one's own libraries. Those libraries will contain information on material and element properties, and can be called by SUBROUTINE during analysis. In this way one can computerize the entire optimization procedure, and decrease design time.

REFERENCES

1. Williams, J. H., and Wang, T. K., "Nondestructive Evaluation of Strength and Seperations Modes in Adhesively Bonded Automotive Glass Fiber Composite Single Lap joints" *Journal of Composite Materials,* Vol. 21, 1987, pp. 14-35.

2. Hart-Smith, L. J., "An Engineer's View Point on Design and Analysis of Aircraft Structural Joints", *Journal of Aerospace Engineering,* Vol. 209, No. 2, 1995, pp. 105-129.

3. Hart-Smith, L. J., "Further Developments in the Design and Analysis of Adhesive-Bonded Structural Joints", *Joining of Composite Materials, ASTM STP 749,* Kedward K. T., Ed., American Society for Testing and Materials, 1981, pp. 3-31.

4. Goland, M. and Reissner, E., "The Stress in Cemented Joints", *Journal of Applied Mechanics,* 1944, pp. A17-A26.

5. Pahoja H. M., "Stress Analysis of an Adhesive Lap joint Subjected to Tension, Shear Force and Bending Moments", *University of Illinois at Urbana-Champaign,* T. & A. M. Report 361, August 1972

6. Vinson, J. R., "Adhesive Bonding of Polymer Composites", *Polymer Engineering Science.*, Vol. 29, 1989, pp.1325-1331.

7. Adams, R. D., "The Mechanics of Bonded Joints", *IMechE,* 1986, pp.17-24.

8. Adams, R. D., "Strength Predictions for Lap Joints Especially with Composite Adherents: A Review", *J. Adhesion,* Vol. 30, 1989, pp.219-242.

9. Lessard, L., "Design of Joints in Composite Structures", *Computer Aided Design for Composite Structures*, S.V. Hoa, Ed., Marcel Dekker Inc., NY, 1995, pp. 273-288.

10. Barthelemy, B. M., Kamat, M. P., and Brinson, H. F., "Finite Element Analysis of Bonded Joints", M. Thesis, Virginia Polytechnic Institute and State University, Blacksburg, Virginia, May 1984.

11. Harris, J. A., and Adams R. D., "Strength prediction for bonded single lap joints by non-linear finite element methods", *International Journal of Adhesion and Adhesives*, Vol. 4, No. 2, 1984, pp. 65-78

12. Adams, R. D., Atkins, R. W., Harris, J. A., "Stress Analysis and Failure Properties of Carbon-Fibre-Reinforced-Plastic/Steel Double Lap Joints", *Journal of Adhesion*, Vol. 20, 1986, pp. 29-53

13. Hildebrand, M., "Non-linear Analysis and Optimization of Adhesively Bonded Single Lap Joints Between Fibre-Reinforced Plastics and Metals", *Int. J. Adhesion and Adhesives*, Vol. 14, No. 4, 1994, pp.261-267.

14. Kairouz, K. C., and Cook, I. P., "The Influence of Bondline Thickness and Overlap Length on the Strength of Bonded Double Lap Composite Joints", *ECCM-8 European Conference on Composite Materials*, Naples, Italy, June 3-6, 1998, Vol. 1, pp.31-38.

15. Tsai, M. Y., and morton J., "Experimental and Numerical Studies of a Laminated Composite Single-lap Adhesive Joint" *Journal of Composite Materials*, Vol. 29, No. 9, 1995, pp. 527-538.

16. Bogy, D. B., "Edge-Bonded Dissimilar Orthogonal Elastic Wedges Under Normal and Sheer Loading', *Journal of Applied Mechanics*, Vol. 35, 1968, pp.460-466.

17. Dunders, J., "Discussion of Edge-Bonded Dissimilar Orthogonal Elastic Wedges Under Normal and Sheer Loading", *Journal of Applied Mechanics*, Vol. 36, 1969, pp.650-652.

18. Bogy, D. B., "Two Edge-Bonded Elastic Wedges of Different Materials and Wedge Angles Under Surface Tractions", *Journal of Applied Mechanics*, Vol. 38, 1971, pp. 377-386.

19. Erdogan, F., "Stress Singularities in a Two-material Wedge", *International Journal of Fracture Mechanics*, Vol. 7, 1971, pp.317-330.

20. Theocaris, P. S., "The Order of Singularity at a Multi-Wedge Corner of Composite Plate", *International Journal of Engineering Science*, Vol. 12, 1974, pp. 107-120.

21. Groth, H. L., "Stress singularities and fracture at interface corners in bonded joints" *Int. J. Adhesion and Adhesives*, April, 1988, pp.107-113.

22. Shorshorov, M. K., and Gukasjan, L.E., "The effect of the Interface Strength on the Strength of the Aluminum-Boron Composite" *Journal of Composite Materials*, Vol. 17, 1983, pp. 527-538.

23. Chapman, G. B. II, "A Nondestructive Method of Evaluating Adhesive Bond Strength in Fiberglass Reinforced Plastic Assemblies", *Joining of Composite Materials, ASTM STP 749*, Kedward K. T., Ed., American Society for Testing and Materials, 1981, pp. 32-60.

24. Hart-Smith, L. J., "The key to Designing Durable Adhesively Bonded Joints", *Composites*, Vol. 25, No. 9, October 1994, pp.895-898.

25. Hart-Smith, L. J., "Adhesive-Bonded Joints for Composites – Phenomenal Considerations", *Proceedings of the Conference on Advanced Composite Technology*, El Segundo, CA, March 1978, pp. 163-180.

26. Renton, W. J., and Vinson, J. R., "The Efficient Design of Adhesive Bonded Joints" " *Journal of Adhesion*, Vol. 7, 1975, pp. 175-193.

27. Greszezuk, L. B., and Macander, A. B., "Static and Fatigue Strength of High Load Intensity Stell-Hybrid Composite Bonded Scarf Joints" *Joining of Composite Materials, ASTM STP 749*, Kedward K. T., Ed., American Society for Testing and Materials, 1981, pp. 75-96.

28. Adams, R. D., and Wake, W. C., "*Structural Adhesive Joints in Engineering*", Elsevier Applied Science Publishers, 1984.

29. Galantucci, L. M., Gravina, A., Chita, G., and Cinquepalmi, M., "Surface treatment for adhesive-bonded joints by excimer laser" *Composites Part A*, Vol.. 27, 1996, pp. 1041-1049

30. Arnold, J. R., and Sanders, C. D., "A Study of Titanium Surface Pretreatments for Bonding With Polyimide and Epoxy Adhesives". *SAMPE Journal*, Vol. 34, No.1, January/February, 1998, pp.11-14.

31. Shokrieh, M. M., "Progressive Fatigue Damage Modeling of Composite Materials", Ph.D. Dissertation, McGill University, February 1996.

32. ABAQUS 5-8-1 Users Manual, Hibbitt, Carlsson & Sorensen. Inc.

33. Loctite Inc., 1001 Trout Brook Crossing, Rocky Hill, CT

34. Amisol Company Ltd., 10500 Cote de Liesse., Suite 115, Lachine, Quebec, H8T 1A4

APPENDIX A

ABAQUS SAMPLE CODE :

(I) SINGLE-LAP JOINT UNDER TENSION, AND

(II) SINGLE-LAP JOINT UNDER OUT-OF-PLANE LOAD

(I) SINGLE-LAP JOINT – BASELINE MODEL IN TENSION

*HEADING
*NODE
1,0.,0.003486
61,.120,0.003486
101,.0,0.00345475
161,.120,0.00345475
201,.0,0.0034235
261,.120,0.0034235
301,.0,0.00339225
361,.120,0.00339225
401,.0,0.003361
461,.120,0.003361
501,.0,0.00332975
561,.120,0.00332975
601,.0,0.0032985
661,.120,0.0032985
701,.0,0.00326725
761,.120,0.00326725
801,.0,0.003236
861,.120,0.003236
901,.0,0.00320475
961,.120,0.00320475
1001,.0,0.0031735
1061,.120,0.0031735
1101,.0,0.00314225
1161,.120,0.00314225
1201,.0,0.003111
1261,.120,0.003111
1301,.0,0.00307975
1361,.120,0.00307975
1401,.0,0.0030485
1461,.120,0.0030485
1501,.0,0.00301725

1561,.120,0.00301725
1601,.0,0.002986
1661,.120,0.002986
1701,.0,0.00295475
1761,.120,0.00295475
1801,.0,0.0029235
1861,.120,0.0029235
1901,.0,0.00289225
1961,.120,0.00289225
2001,.0,0.002861
2061,.120,0.002861
2101,.0,0.00282975
2161,.120,0.00282975
2201,.0,0.0027985
2261,.120,0.0027985
2301,.0,0.00276725
2361,.120,0.00276725
2401,.0,0.002736
2461,.120,0.002736
2501,.0,0.00270475
2561,.120,0.00270475
2601,.0,0.0026735
2661,.120,0.0026735
2701,.0,0.00264225
2761,.120,0.00264225
2801,.0,0.00261100
2861,.120,0.00261100
2901,.0,0.00257975
2961,.120,0.00257975
3001,.0,0.0025485
3061,.120,0.0025485
3101,.0,0.00251725
3161,.120,0.00251725
3201,.0,0.002486
3261,.120,0.002486
3301,.100,0.0024735
3321,.120,0.0024735

3401,.100,0.002461
3421,.120,0.002461
3501,.100,0.0024485
3521,.120,0.0024485
3601,.100,0.002436
3621,.120,0.002436
3701,.100,0.0024235
3721,.120,0.0024235
3801,.100,0.002411
3821,.120,0.002411
3901,.100,0.0023985
3921,.120,0.0023985
4001,.100,0.002386
4021,.120,0.002386
4101,.100,0.0023735
4121,.120,0.0023735
4201,.100,0.002361
4221,.120,0.002361
4301,.100,0.0023485
4321,.120,0.0023485
4401,.100,0.002336
4461,.220,0.002336
4501,.100,0.002263
4561,.220,0.002263
4601,.100,0.00219
4661,.220,0.00219
4701,.100,0.002117
4761,.220,0.002117
4801,.100,0.002044
4861,.220,0.002044
4901,.100,0.001971
4961,.220,0.001971
5001,.100,0.001898
5061,.220,0.001898
5101,.100,0.001825
5161,.220,0.001825
5201,.100,0.001752

5261,.220,0.001752
5301,.100,0.001679
5361,.220,0.001679
5401,.100,0.001606
5461,.220,0.001606
5501,.100,0.001533
5561,.220,0.001533
5601,.100,0.00146
5661,.220,0.00146
5701,.100,0.001387
5761,.220,0.001387
5801,.100,0.001314
5861,.220,0.001314
5901,.100,0.001241
5961,.220,0.001241
6001,.100,0.001168
6061,.220,0.001168
6101,.100,0.001095
6161,.220,0.001095
6201,.100,0.001022
6261,.220,0.001022
6301,.100,0.000949
6361,.220,0.000949
6401,.100,0.000876
6461,.220,0.000876
6501,.100,0.000803
6561,.220,0.000803
6601,.100,0.000730
6661,.220,0.000730
6701,.100,0.000657
6761,.220,0.000657
6801,.100,0.000584
6861,.220,0.000584
6901,.100,0.000511
6961,.220,0.000511
7001,.100,0.000438
7061,.220,0.000438

7101,.100,0.000365
7161,.220,0.000365
7201,.100,0.000292
7261,.220,0.000292
7301,.100,0.000219
7361,.220,0.000219
7401,.100,0.000146
7461,.220,0.000146
7501,.100,0.000073
7561,.220,0.000073
7601,.100,.0
7661,.220,.0
8000,.220,0.001168
*NGEN
1,61
101,161,2
201,261
301,361,2
401,461
501,561,2
601,661
701,761,2
801,861
901,961,2
1001,1061
1101,1161,2
1201,1261
1301,1361,2
1401,1461
1501,1561,2
1601,1661
1701,1761,2
1801,1861
1901,1961,2
2001,2061
2101,2161,2
2201,2261

2301,2361,2
2401,2461
2501,2561,2
2601,2661
2701,2761,2
2801,2861
2901,2961,2
3001,3061
3101,3161,2
3201,3261
3301,3321,2
3401,3421
3501,3521,2
3601,3621
3701,3721,2
3801,3821
3901,3921,2
4001,4021
4101,4121,2
4201,4221
4301,4321,2
4401,4461
4501,4561,2
4601,4661
4701,4761,2
4801,4861
4901,4961,2
5001,5061
5101,5161,2
5201,5261
5301,5361,2
5401,5461
5501,5561,2
5601,5661
5701,5761,2
5801,5861
5901,5961,2

```
6001,6061
6101,6161,2
6201,6261
6301,6361,2
6401,6461
6501,6561,2
6601,6661
6701,6761,2
6801,6861
6901,6961,2
7001,7061
7101,7161,2
7201,7261
7301,7361,2
7401,7461
7501,7561,2
7601,7661
*NSET,NSET=BONDL
1,101,201,301,401,501,601,701,801,901,
1001,1101,1201,1301,1401,1501,1601,1701,
1801,1901,2001,2101,2201,2301,2401,2501,
2601,2701,2801,2901,3001,3101,3201
*NSET,NSET=BONDR
4460,4461,7660,7661,1,2,3201,3202
*ELEMENT,TYPE=RAX2
8001,4461,4561
*ELGEN,ELSET=RIGID
8001,32,100
*RIGID BODY,ELSET=RIGID,REF NODE=8000
*ELEMENT,TYPE=CPE8R,ELSET=TOP1
1,201,203,3,1,202,103,2,101
*ELGEN,ELSET=TOP1
1,30,2,1
*ELEMENT,TYPE=CPE8R,ELSET=TOP2
41,401,403,203,201,402,303,202,301
*ELGEN,ELSET=TOP2
41,30,2,1
```

```
*ELEMENT,TYPE=CPE8R,ELSET=TOP3
81,601,603,403,401,602,503,402,501
*ELGEN,ELSET=TOP3
81,30,2,1
*ELEMENT,TYPE=CPE8R,ELSET=TOP4
121,801,803,603,601,802,703,602,701
*ELGEN,ELSET=TOP4
121,30,2,1
*ELEMENT,TYPE=CPE8R,ELSET=TOP5
161,1001,1003,803,801,1002,903,802,901
*ELGEN,ELSET=TOP5
161,30,2,1
*ELEMENT,TYPE=CPE8R,ELSET=TOP6
201,1201,1203,1003,1001,1202,1103,1002,1101
*ELGEN,ELSET=TOP6
201,30,2,1
*ELEMENT,TYPE=CPE8R,ELSET=TOP7
241,1401,1403,1203,1201,1402,1303,1202,1301
*ELGEN,ELSET=TOP7
241,30,2,1
*ELEMENT,TYPE=CPE8R,ELSET=TOP8
281,1601,1603,1403,1401,1602,1503,1402,1501
*ELGEN,ELSET=TOP8
281,30,2,1
*ELEMENT,TYPE=CPE8R,ELSET=TOP9
321,1801,1803,1603,1601,1802,1703,1602,1701
*ELGEN,ELSET=TOP9
321,30,2,1
*ELEMENT,TYPE=CPE8R,ELSET=TOP10
361,2001,2003,1803,1801,2002,1903,1802,1901
*ELGEN,ELSET=TOP10
361,30,2,1
*ELEMENT,TYPE=CPE8R,ELSET=TOP11
401,2201,2203,2003,2001,2202,2103,2002,2101
*ELGEN,ELSET=TOP11
401,30,2,1
*ELEMENT,TYPE=CPE8R,ELSET=TOP12
```

```
441,2401,2403,2203,2201,2402,2303,2202,2301
*ELGEN,ELSET=TOP12
441,30,2,1
*ELEMENT,TYPE=CPE8R,ELSET=TOP13
481,2601,2603,2403,2401,2602,2503,2402,2501
*ELGEN,ELSET=TOP13
481,30,2,1
*ELEMENT,TYPE=CPE8R,ELSET=TOP14
521,2801,2803,2603,2601,2802,2703,2602,2701
*ELGEN,ELSET=TOP14
521,30,2,1
*ELEMENT,TYPE=CPE8R,ELSET=TOP15
561,3001,3003,2803,2801,3002,2903,2802,2901
*ELGEN,ELSET=TOP15
561,30,2,1
*ELEMENT,TYPE=CPE8R,ELSET=TOP16
601,3201,3203,3003,3001,3202,3103,3002,3101
*ELGEN,ELSET=TOP16
601,30,2,1
*ELEMENT,TYPE=CPE8R,ELSET=MID1
1001,3401,3403,3243,3241,3402,3303,3242,3301
*ELGEN,ELSET=MID1
1001,10,2,1
*ELEMENT,TYPE=CPE8R,ELSET=MID2
1021,3601,3603,3403,3401,3602,3503,3402,3501
*ELGEN,ELSET=MID2
1021,10,2,1
*ELEMENT,TYPE=CPE8R,ELSET=MID3
1041,3801,3803,3603,3601,3802,3703,3602,3701
*ELGEN,ELSET=MID3
1041,10,2,1
*ELEMENT,TYPE=CPE8R,ELSET=MID4
1061,4001,4003,3803,3801,4002,3903,3802,3901
*ELGEN,ELSET=MID4
1061,10,2,1
*ELEMENT,TYPE=CPE8R,ELSET=MID5
1081,4201,4203,4003,4001,4202,4103,4002,4101
```

```
*ELGEN,ELSET=MID5
1081,10,2,1
*ELEMENT,TYPE=CPE8R,ELSET=MID6
1101,4401,4403,4203,4201,4402,4303,4202,4301
*ELGEN,ELSET=MID6
1101,10,2,1
*ELEMENT,TYPE=CPE8R,ELSET=BOT1
2001,4601,4603,4403,4401,4602,4503,4402,4501
*ELGEN,ELSET=BOT1
2001,30,2,1
*ELEMENT,TYPE=CPE8R,ELSET=BOT2
2041,4801,4803,4603,4601,4802,4703,4602,4701
*ELGEN,ELSET=BOT2
2041,30,2,1
*ELEMENT,TYPE=CPE8R,ELSET=BOT3
2081,5001,5003,4803,4801,5002,4903,4802,4901
*ELGEN,ELSET=BOT3
2081,30,2,1
*ELEMENT,TYPE=CPE8R,ELSET=BOT4
2121,5201,5203,5003,5001,5202,5103,5002,5101
*ELGEN,ELSET=BOT4
2121,30,2,1
*ELEMENT,TYPE=CPE8R,ELSET=BOT5
2161,5401,5403,5203,5201,5402,5303,5202,5301
*ELGEN,ELSET=BOT5
2161,30,2,1
*ELEMENT,TYPE=CPE8R,ELSET=BOT6
2201,5601,5603,5403,5401,5602,5503,5402,5501
*ELGEN,ELSET=BOT6
2201,30,2,1
*ELEMENT,TYPE=CPE8R,ELSET=BOT7
2241,5801,5803,5603,5601,5802,5703,5602,5701
*ELGEN,ELSET=BOT7
2241,30,2,1
*ELEMENT,TYPE=CPE8R,ELSET=BOT8
2281,6001,6003,5803,5801,6002,5903,5802,5901
*ELGEN,ELSET=BOT8
```

```
2281,30,2,1
*ELEMENT,TYPE=CPE8R,ELSET=BOT9
2321,6201,6203,6003,6001,6202,6103,6002,6101
*ELGEN,ELSET=BOT9
2321,30,2,1
*ELEMENT,TYPE=CPE8R,ELSET=BOT10
2361,6401,6403,6203,6201,6402,6303,6202,6301
*ELGEN,ELSET=BOT10
2361,30,2,1
*ELEMENT,TYPE=CPE8R,ELSET=BOT11
2401,6601,6603,6403,6401,6602,6503,6402,6501
*ELGEN,ELSET=BOT11
2401,30,2,1
*ELEMENT,TYPE=CPE8R,ELSET=BOT12
2441,6801,6803,6603,6601,6802,6703,6602,6701
*ELGEN,ELSET=BOT12
2441,30,2,1
*ELEMENT,TYPE=CPE8R,ELSET=BOT13
2481,7001,7003,6803,6801,7002,6903,6802,6901
*ELGEN,ELSET=BOT13
2481,30,2,1
*ELEMENT,TYPE=CPE8R,ELSET=BOT14
2521,7201,7203,7003,7001,7202,7103,7002,7101
*ELGEN,ELSET=BOT14
2521,30,2,1
*ELEMENT,TYPE=CPE8R,ELSET=BOT15
2561,7401,7403,7203,7201,7402,7303,7202,7301
*ELGEN,ELSET=BOT15
2561,30,2,1
*ELEMENT,TYPE=CPE8R,ELSET=BOT16
2601,7601,7603,7403,7401,7602,7503,7402,7501
*ELGEN,ELSET=BOT16
2601,30,2,1
*ELSET,ELSET=TOP
TOP1,TOP2,TOP3,TOP4,TOP5,TOP6,TOP7,TOP8,
TOP9,TOP10,TOP11,TOP12,TOP13,TOP14,TOP15,TOP16
*ELSET,ELSET=MID
```

```
MID1,MID2,MID3,MID4,
MID5,MID6
*ELSET,ELSET=BOT0
BOT1,BOT2,BOT3,BOT4,
BOT13,BOT14,BOT15,BOT16
*ELSET,ELSET=BOT90
BOT5,BOT6,BOT7,BOT8,
BOT9,BOT10,BOT11,BOT12
*SOLID SECTION,ELSET=TOP,MATERIAL=MAT1
0.02525
*MATERIAL,NAME=MAT1
*ELASTIC,TYPE=ENGINEERING CONSTANTS
113.76E9, 113.76E9, 113.76E9, 0.33, 0.33, 0.33, 42.768E9,42.768E9,
42.768E9
*SOLID SECTION,ELSET=MID,MATERIAL=MAT2
0.02525
*MATERIAL,NAME=MAT2
*ELASTIC,TYPE=ENGINEERING CONSTANTS
689.48E6, 689.48E6, 689.48E6, 0.33, 0.33, 0.33,259.203E6,259.203E6,
259.203E6
*SOLID SECTION,ELSET=BOT0,MATERIAL=MAT3
0.02525
*MATERIAL,NAME=MAT3
*ELASTIC,TYPE=ENGINEERING CONSTANTS
147.0E9, 9.0E9, 9.0E9, 0.3, 0.3, 0.42, 5.0E9,5.0E9,
3.0E9
*SOLID SECTION,ELSET=BOT90,MATERIAL=MAT4
0.02525
*MATERIAL,NAME=MAT4
*ELASTIC,TYPE=ENGINEERING CONSTANTS
9.0E9, 9.0E9, 9.0E9, 0.3, 0.3, 0.42, 5.0E9,5.0E9,
3.0E9
*BOUNDARY
BONDL,1
BONDR,2
*RESTART,WRITE,FREQUENCY=70
*STEP,NLGEOM,INC=1000000000
```

```
*STATIC,DIRECT
.1,7.0
*CLOAD
8000,1,4000
*ENERGY PRINT,ELSET=MID,FREQUENCY=70
*NODE PRINT,FREQUENCY=70
U,
RF,
CF
*EL PRINT,FREQUENCY=70
*NODE FILE,FREQUENCY=70
U,
RF,
CF
*END STEP
```

(II) SINGLE-LAP JOINT – BASELINE MODEL IN BENDING

In the bending case, the ABAQUS input file has different loading and boundary conditions than the tension input file, and therefore only this part of the model is introduced.

```
*BOUNDARY
9,1,2
4453,2
*RESTART,WRITE,FREQUENCY=70
*STEP,NLGEOM,INC=1000000000
*STATIC,DIRECT
.1,7.0
*CLOAD
7611,2,109
```